© 2016. Published by The Company of Biologists Ltd | Journal of Cell Science (2016) 129, 3803-3815 doi:10.1242/jcs.189191

RESEARCH ARTICLE

Mature lipid droplets are accessible to ER luminal proteins

Shirish Mishra, Rasha Khaddaj, Stéphanie Cottier, Vendula Stradalova, Claire Jacob and Roger Schneiter*

ABSTRACT

Lipid droplets are found in most organisms where they serve to store energy in the form of neutral lipids. They are formed at the endoplasmic reticulum (ER) membrane where the neutral-lipid-synthesizing enzymes are located. Recent results indicate that lipid droplets remain functionally connected to the ER membrane in yeast and mammalian cells to allow the exchange of both lipids and integral membrane proteins between the two compartments. The precise nature of the interface between the ER membrane and lipid droplets, however, is still ill-defined. Here, we probe the topology of lipid droplet biogenesis by artificially targeting proteins that have high affinity for lipid droplets to inside the luminal compartment of the ER. Unexpectedly, these proteins still localize to lipid droplets in both yeast and mammalian cells, indicating that lipid droplets are accessible from within the ER lumen. These data are consistent with a model in which lipid droplets form a specialized domain in the ER membrane that is accessible from both the cytosolic and the ER luminal side.

KEY WORDS: Lipid storage, Triacylglycerol, Endoplasmic reticulum, Membrane topology, Perilipins

INTRODUCTION

Lipid droplets serve to store metabolic energy in the form of neutral lipids, particularly triacylglycerols and steryl esters. They form globular intracellular structures composed of a core of neutral lipids that is covered by a phospholipid monolayer harboring a limited set of proteins, many of which are important for neutral lipid synthesis or breakdown. However, triacylglycerols and steryl esters are synthesized by endoplasmic reticulum (ER)-localized enzymes. This observation supports a model of lipid droplet biogenesis in which neutral lipids first accumulate between the two leaflets of the ER membrane. These lipid lenses then grow in size and mature in their protein composition to form nascent lipid droplets, which are then postulated to bud from the ER membrane to form cytosolic structures (Ohsaki et al., 2014; Pol et al., 2014; Thiam et al., 2013).

Lipid droplets are closely associated with different cellular organelles including mitochondria, vacuoles, peroxisomes and ER (Barbosa et al., 2015; Murphy et al., 2009). The association of lipid droplets with the ER has been extensively investigated. Live-cell microscopy has shown close association of lipid droplets with the ER membrane and concurrent movement of the two structures (Szymanski et al., 2007; Targett-Adams et al., 2003). Freeze fracture experiments have revealed that the ER membrane is continuous with the surface layer of lipid droplets or that it encloses lipid droplets tightly (Blanchette-Mackie et al., 1995; Robenek et al., 2006). Functional studies have indicated that the activation of fatty acids and their incorporation into triacylglycerol occurs at specific ER microdomains from where lipid droplets grow (Kassan et al., 2013; Xu et al., 2012b). The contact sites between the ER and lipid droplets have also been characterized and shown to be stabilized by the seipin complex, which acts as a diffusion barrier between the two compartments (Grippa et al., 2015).

Both proteins and lipids can be exchanged between the ER and lipid droplets and this process is dynamically regulated. Neutral lipid accumulation induces relocalization of integral membrane proteins from the ER to lipid droplets, and these proteins move again back into the ER when neutral lipid pools are degraded (Jacquier et al., 2011; Kassan et al., 2013; Wilfling et al., 2013; Zehmer et al., 2009). In addition, intermediates of neutral lipid synthesis and degradation are shuffled between the two compartments to allow growth and shrinkage of lipid droplets, depending on the metabolic needs of the cell (Markgraf et al., 2014). Moreover, lipid droplet size is controlled by the exchange of neutral lipids between lipid droplets, a process that is mediated by members of the CIDE family (Xu et al., 2012a).

The fact that one of the two triacylglycerol biosynthetic enzymes in yeast, Lro1, an integral membrane enzyme of the ER, has its active site positioned within the ER lumen indicates that neutral lipids can be formed in the inner leaflet of the ER membrane and reach nascent, or possibly even mature, lipid droplets (Choudhary et al., 2011). Moreover, lipid droplets accumulating triacylglycerol formed by Lro1 are seemingly indistinguishable from those having neutral lipids formed by the acyl-CoA-dependent acyltransferase Dga1 (Sandager et al., 2002; Sorger et al., 2004). These observations, together with the fact that lipoproteins of animal cells, which are structurally very similar to lipid droplets, mature and assemble within the ER lumen from where they are then secreted into the extracellular space, prompted us to investigate the topology of lipid droplet formation in more detail (Fisher and Ginsberg, 2002; Hussain et al., 2003). Although it is clear that lipid droplets are accessible to soluble cytosolic factors, such as the perilipins (PLINs), which are abundant structural proteins that are targeted to the lipid droplets through conserved amphipathic helices, it is unknown whether lipid droplets are also accessible from within the lumen of the ER (Rowe et al., 2016).

Here, we probe the topological relationship between lipid droplets and the ER by targeting cytosolic lipid droplet marker proteins into the lumen of the ER. Remarkably, these ER luminal probes are still capable of localizing to lipid droplets, indicating that lipid droplets are accessible from within the ER luminal compartment. These results suggest that lipid droplets represent a domain within the ER that is accessible from both the cytosolic and the luminal site. A model for the biogenesis of lipid droplets that is consistent with these observations is discussed.

University of Fribourg, Department of Biology, Fribourg 1700, Switzerland.

*Author for correspondence (roger.schneiter@unifr.ch)

R.S., 0000-0002-9102-8396

Received 11 March 2016; Accepted 17 August 2016

Journal of Cell Science (2016) 129, 3803-3815 doi:10.1242/jcs.189191

RESULTS

The lipid droplet marker proteins Erg6 and Tgl1 still localize to lipid droplets when they contain an N-terminal signal sequence

To probe the topology of lipid droplet formation, we targeted lipid-droplet-resident proteins into the ER lumen and examined their subcellular distribution. Therefore, two yeast lipid droplet marker proteins, Erg6, an enzyme of the ergosterol biosynthetic pathway, and Tgl1, a steryl ester lipase, were fused to the signal sequence of Pry1 (amino acids 1 to 19), a secreted glycoprotein (Choudhary and Schneiter, 2012; Koffel et al., 2005; Leber et al., 1994). The localization of GFP-tagged versions of these proteins was then analyzed by confocal microscopy. Given that Tgl1 contains an N-terminal transmembrane domain, we fused a truncated version lacking the first 29 amino acids (Tgl1Δtm) to the signal sequence of Pry1 (Koffel et al., 2005). The native versions of Erg6 and the cytosolic version of Tgl1 lacking the transmembrane domain localized to punctate structures that co-stained with Nile Red, a lipophilic dye that stains lipid droplets, indicating that both reporter proteins localize to lipid droplets. Unexpectedly, the signal-sequence-containing versions of these proteins, denoted ss-Erg6 and ss-Tgl1(Δtm), also showed a punctate pattern and the GFP signal merged with Nile-Red-stained lipid droplets, indicating that the presence of the ER signal sequence allows proper targeting of these proteins to lipid droplets (Fig. 1A).

The synthesis of neutral lipids in yeast is under the control of four enzymes, two of which, Dga1 and Lro1, produce triacylglycerols, and the other two of which, Are1 and Are2, generate steryl esters (Czabany et al., 2007). Cells lacking all four neutral-lipid-synthesizing enzymes are devoid of lipid droplets (Sandager et al., 2002). In the absence of lipid droplets, many of the otherwise lipid-droplet-localized proteins relocalize to the ER membrane (Jacquier et al., 2011; Kassan et al., 2013; Wilfling et al., 2013; Zehmer et al., 2009). To test whether the signal-sequence-containing reporter proteins would also localize to the ER membrane in cells lacking lipid droplets, their subcellular localization was analyzed in an inducible strain in which three of the genes required for neutral lipid synthesis (*ARE1*, *ARE2* and *DGA1*) were deleted and the fourth gene was placed under transcriptional control of a glucose repressible promoter (*GAL-LRO1*). Under conditions where *LRO1* is repressed, Erg6 and Tgl1(Δtm) and the signal-sequence-containing reporters ss-Erg6 and ss-Tgl1(Δtm), displayed a circular staining that merged with the localization of the ER luminal marker protein ss-mCherry-HDEL, indicating that signal-sequence-containing proteins relocalize to the ER in cells that have no lipid droplets (Rogers et al., 2014) (Fig. 1B). Thus, signal-sequence-containing lipid droplet proteins

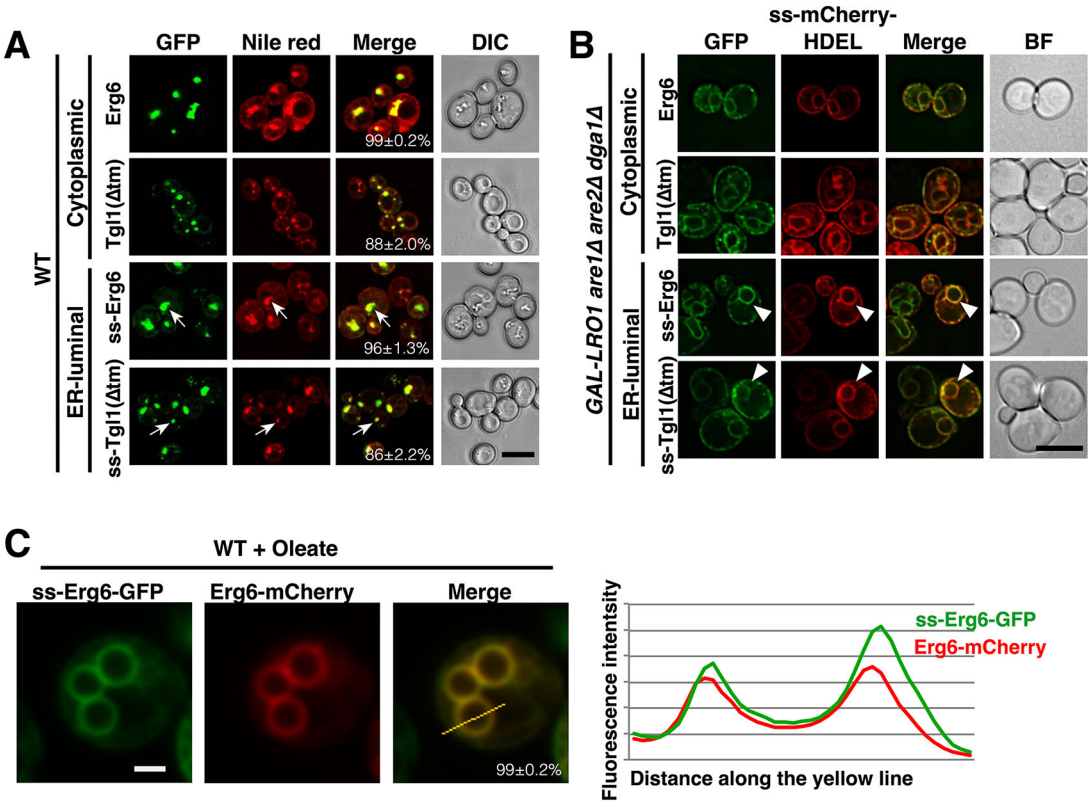

Fig. 1. Yeast endogenous lipid droplet proteins containing an ER signal sequence localize to lipid droplets. (A) Wild-type (WT) cells expressing GFP-tagged lipid droplet marker proteins Erg6 or Tgl1(Δtm) and cells expressing signal-sequence-containing versions of these proteins, ss-Erg6 or ss-Tgl1(Δtm), were stained with the lipophilic dye Nile Red, and colocalization was analyzed by confocal microscopy (arrows). The degree of colocalization of the respective GFP-tagged protein with the lipid droplet marker Erg6–mCherry is indicated by the percentages (mean±s.e.m.; *n*>100 cells). Differential interference contrast (DIC) images are shown to the right. Scale bar: 5 µm. (B) GFP-tagged lipid droplet marker proteins label the ER in cells lacking lipid droplets. The localization of the indicated GFP-tagged lipid droplet proteins and the ER marker protein ss-mCherry-HDEL were analyzed by fluorescence microscopy. Colocalization in the perinuclear ER is indicated by arrowheads. Bright-field (BF) images of the cells are shown to the right. Scale bar: 5 µm. (C) Colocalization of ss-Erg6–GFP and Erg6–mCherry. WT cells expressing the indicated fluorescent proteins were cultivated in medium containing oleate and analyzed by confocal microscopy. The degree of colocalization of the two proteins is 99±1% (mean±s.e.m.; *n*>100 cells). The graph shows fluorescence intensity profiles along the yellow line. Scale bar: 1 µm.

Journal of Cell Science (2016) 129, 3803-3815 doi:10.1242/jcs.189191

behave similar to the non signal-sequence-containing counterparts in that they localized to lipid droplets in cells that made neutral lipids, whereas in the absence of lipid droplets the proteins localized to the ER.

To examine the localization of ss-Erg6 on lipid droplets that are labeled by a lipid-droplet-resident protein instead of Nile Red, we generated a strain that expressed a GFP-tagged version of ss-Erg6 and an mCherry-tagged version of wild-type Erg6. Cells were cultivated in medium containing oleate to increase the size of lipid droplet. Both proteins displayed circular rim labeling on these large lipid droplets. The fluorescence intensity along a line crossing one of these large lipid droplets reveals extensive overlap between the localization of ss-Erg6 and Erg6, and more than 99% of the lipid droplets were co-stained with both ss-Erg6–GFP and Erg6–mCherry (Fig. 1C). Similarly, cytosolic and signal-sequence-containing versions of Erg6 and Tgl1(Δtm) displayed a high degree (>86%) of colocalization with lipid droplets marked by Erg6–mCherry in cells grown in rich medium (Fig. 1A).

Signal-sequence-containing perilipins are targeted to the ER lumen and localize to lipid droplets

Erg6 and Tgl1 are both membrane-associated proteins; thus, we wondered whether a truly cytosolic lipid droplet protein could also be targeted to lipid droplets from within the ER luminal compartment. Therefore, we tested whether addition of a signal sequence from the secreted glycoprotein Pry1 (amino acids 1 to 19) to the human lipid-droplet-scaffolding proteins PLIN1–PLIN3, would also result in targeting of the proteins to lipid droplets. PLINs constitute a family of related proteins, sharing a common PAT domain, originally identified in the founding members of that family, PLIN1, PLIN2 (also known as adipophilin, ADRP) and PLIN3 (also known as TIP47) (Bickel et al., 2009; Miura et al., 2002). PLINs are properly targeted to lipid droplets when expressed in yeast, and they are soluble proteins in cells that lack the capacity to form lipid droplets (Jacquier et al., 2013). When fused to the signal sequence of Pry1, all three PLINs localized to Nile-Red-positive punctate structures, indicating that even soluble proteins when targeted into the ER lumen localize to lipid droplets (Fig. 2A).

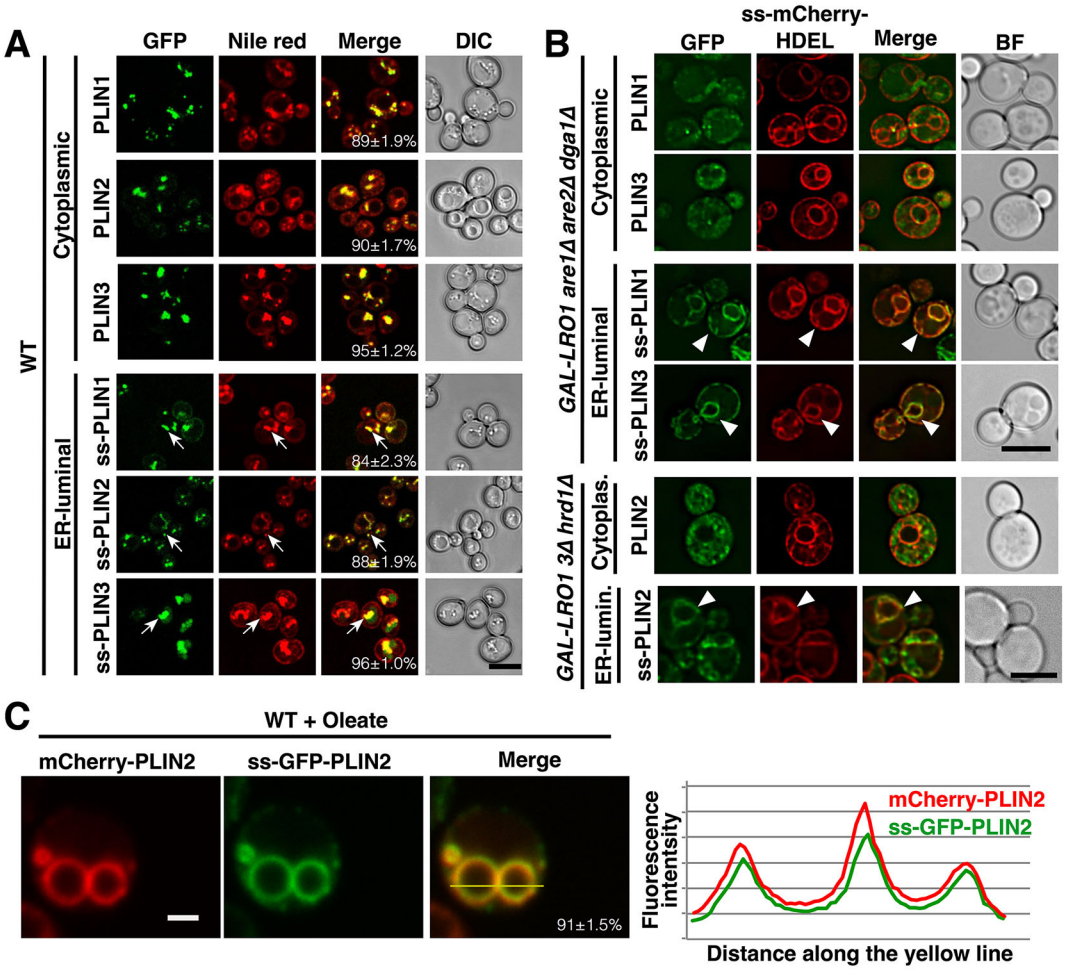

Fig. 2. Mammalian PLINs localize to yeast lipid droplets even when targeted to the ER lumen. (A) Cells expressing cytosolic and signal-sequence-containing (ss-) versions of mammalian PLINs (PLIN1–PLIN3) were stained with Nile Red and colocalization was analyzed by confocal microscopy (arrows). The degree of colocalization with the lipid droplet marker Erg6–mCherry is indicated by the percentages (mean±s.e.m.; *n*>100 cells). Scale bar: 5 µm. (B) Localization of PLIN1, PLIN3, ss-PLIN1 and ss-PLIN3 in cells lacking lipid droplets (*GAL-LRO1 are1Δ are2Δ dga1Δ*) and expressing the ER luminal marker ss-mCherry-HDEL. Localization of PLIN2 and ss-PLIN2 in cells lacking lipid droplets and the ubiquitin-protein ligase Hrd1 (*GAL-LRO1 are1Δ are2Δ dga1Δ hrd1Δ*). Circular labeling of the perinuclear and cortical ER by ss-PLINs is indicated by arrowheads. Scale bar: 5 µm. (C) Colocalization of ss-GFP–PLIN2 and the cytosolic mCherry–PLIN2. Wild-type (WT) cells expressing the indicated fluorescent proteins were cultivated in medium containing oleate and analyzed by confocal microscopy. The degree of colocalization of the two proteins is 91±9% (mean±s.e.m.; *n*>100 cells). The graph shows fluorescence intensity profiles along the yellow line. Scale bar: 1 µm.

Journal of Cell Science (2016) 129, 3803-3815 doi:10.1242/jcs.189191

Both cytosolic and signal-sequence-containing versions of these PLINs (denoted ss-PLIN1, ss-PLIN2 and ss-PLIN3) also displayed a high degree (>84%) of colocalization with lipid droplets marked by Erg6–mCherry (Fig. 2A).

To confirm that the appended signal sequence effectively targeted the PLINs into the ER lumen, we analyzed their subcellular distribution in cells lacking lipid droplets. Expression of PLINs in cells lacking neutral lipids, profoundly affected their subcellular localization. Instead of showing a punctate lipid droplet localization as observed in wild-type cells, the cytosolic PLINs showed a diffuse cytosolic distribution (Jacquier et al., 2013) (Fig. 2B). In marked contrast, ss-PLIN1 and ss-PLIN3 displayed ring-like staining and colocalized with the ER luminal marker ss-mCherry-HDEL (Fig. 2B). ss-PLIN2 was hardly detectable when expressed in cells lacking lipid droplets, possibly because the protein was rapidly degraded. To visualize its localization in cell lacking lipid droplets, we deleted Hrd1, a ubiquitin protein ligase required for ER-associated degradation (ERAD) of misfolded ER luminal proteins (Carvalho et al., 2006). Whereas cytosolic PLIN2 displayed cytosolic localization in cells lacking lipid droplets, ss-PLIN2 displayed ER staining in a *hrd1*Δ mutant background (Fig. 2B). These results indicate that ss-PLINs are localized to the lumen of the ER in cells that have no lipid droplets and that these ER luminal proteins can reach and localize to lipid droplets when cells have lipid droplets.

To examine the localization of ss-PLIN2 on lipid droplets that are labeled by a lipid-droplet-resident protein instead of Nile Red, we generated a strain that expressed a GFP-tagged version of ss-PLIN2 and an mCherry-tagged version of cytosolic PLIN2. Cells were again cultivated in medium containing oleate to increase the size of lipid droplet. Both proteins displayed circular rim staining on these large lipid droplets. The fluorescence intensity along a line crossing two of these large lipid droplets revealed extensive overlap between the localization of cytosolic PLIN2 and the ER luminal ss-PLIN2, and more than 91% of the lipid droplets were co-stained with both markers (Fig. 2C).

Signal-sequence-containing reporter proteins are glycosylated and protected from protease degradation

Next, targeting of the signal-sequence-containing marker proteins into the ER lumen was assessed by western blotting. Whereas the cytosolic version of Erg6–GFP essentially ran as a discrete band at its expected molecular mass (~70 kDa), ss-Erg6–GFP migrated as two bands of higher molecular mass, irrespective of whether the protein was expressed in wild-type cells or in cells lacking lipid droplets (Fig. 3A). Analysis of the primary sequence of Erg6 revealed the presence of two predicted N-glycosylation sites, suggesting that the high-molecular-mass bands observed in ss-Erg6 are due to N-linked glycosylation of the protein, a posttranslational modification that is confined to the luminal compartment of the ER. PLIN2 and PLIN3, by contrast, had no predicted N-glycosylation sites, but their signal-sequence-containing versions still ran as multiple bands with lower electrophoretic mobility compared to their cytosolic versions, suggesting that these ss-PLINs are subject to O-linked glycosylation. Accordingly, treatment of cell lysates with endoglycosidase H, which removes N-linked glycans, resulted in a downshift of ss-Erg6 and of that of a glycosylated ER protein, Wbp1, a subunit of the oligosaccharyl transferase complex, which served as a control for the endoglycosidase treatment (Fig. 3B). The migration of ss-PLIN2 and ss-PLIN3, however, was unaffected (Fig. 3B). By contrast, treatment with trifluoromethanesulfonic acid (TFMS), which cleaves O-glycosidic bonds, resulted in the conversion of the slow-migrating forms of ss-PLIN2 and ss-PLIN3 into faster migrating forms of these proteins (Fig. 3C). TFMS treatment also converted the high-molecular-mass form of Gas1 (130 kDa), a glycosylphosphatidylinositol (GPI)-linked cell surface protein, into its deglycosylated form (~105 kDa). Tgl1(Δtm) and PLIN1 were not included into these studies, because the cytosolic and signal-sequence-containing variants of these proteins migrated as a single band upon separation by SDS-PAGE, indicating that the translocated versions of these proteins were not subject to posttranslational modifications (data not shown). Taken together, these results show that ss-Erg6, ss-PLIN2 and ss-PLIN3 are subject to glycosylation, and hence are translocated into the luminal compartment of the ER.

To further confirm that the signal-sequence-containing reporter proteins are present in the ER lumen, we isolated microsomes and tested whether the proteins would be accessible to degradation by proteinase K. Consistent with a cytosolic accessibility of Erg6, Tgl1(Δtm) and PLIN1–PLIN3, these proteins were rapidly degraded upon incubation of microsomes with proteinase K (Fig. 3D). The signal-sequence-containing versions of these proteins, however, were protected from proteinase K degradation and they became protease sensitive only upon addition of detergents, demonstrating that these proteins are in a luminal compartment. The ER luminal chaperone Kar2 was degraded only after detergent addition, showing that microsomes were intact during the experiments. Proteinase K accessibility of ss-Erg6 and ss-PLIN3 was independent of whether the cells contained lipid droplets or not. This indicates that the circular ER labeling observed in Figs 1B and 2B in cells lacking lipid droplets is indeed due to an ER luminal localization rather than an association of these proteins with the membrane periphery (Fig. S1A).

To test whether the signal-sequence-containing lipid-droplet-localized markers were also enriched on lipid droplets, we performed subcellular fractionation and isolated lipid droplets by flotation on Ficoll density gradients. ss-Erg6 and ss-Tgl1(Δtm) were enriched on isolated lipid droplets to a similar degree, as were the corresponding non signal-sequence-containing proteins Erg6, Tgl1(Δtm) and Ayr1, a marker protein for lipid droplets (Athenstaedt and Daum, 2000) (Fig. 3E). We have previously shown that the cytosolic PLINs are greatly enriched on isolated lipid droplets when expressed in yeast (Jacquier et al., 2013). A similar result was found for the signal-sequence-containing PLIN1–PLIN3 proteins (Fig. 3E).

To examine whether it is indeed the glycosylated forms of these proteins that are enriched on lipid droplets, we compared the migration of the cytosolic versions of Erg6, PLIN2 and PLIN3 to their ER luminal versions isolated from lipid droplets. ss-Erg6, ss-PLIN2 and ss-PLIN3 from isolated lipid droplets showed bands of higher molecular mass compared to their cytosolic variants, indicating that the glycosylated versions of these ER luminal proteins are enriched on lipid droplets (Fig. 3F).

Signal-sequence-containing reporter proteins are efficiently targeted into the ER lumen

To address the possibility that the signal-sequence-containing proteins are inefficiently translocated into the ER lumen or that they get retro-translocated back into the cytosol resulting in an lipid droplet labeling due to trace amounts of these proteins in the cytosol, we fused them to an *in vivo* dual topology reporter system composed of a fusion between the hemagglutinin (HA) epitope, invertase (*SUC2*) and *HIS4C* (Kim et al., 2003b). *HIS4C* encodes histidinol dehydrogenase, which catalyzes the conversion of

Journal of Cell Science (2016) 129, 3803-3815 doi:10.1242/jcs.189191

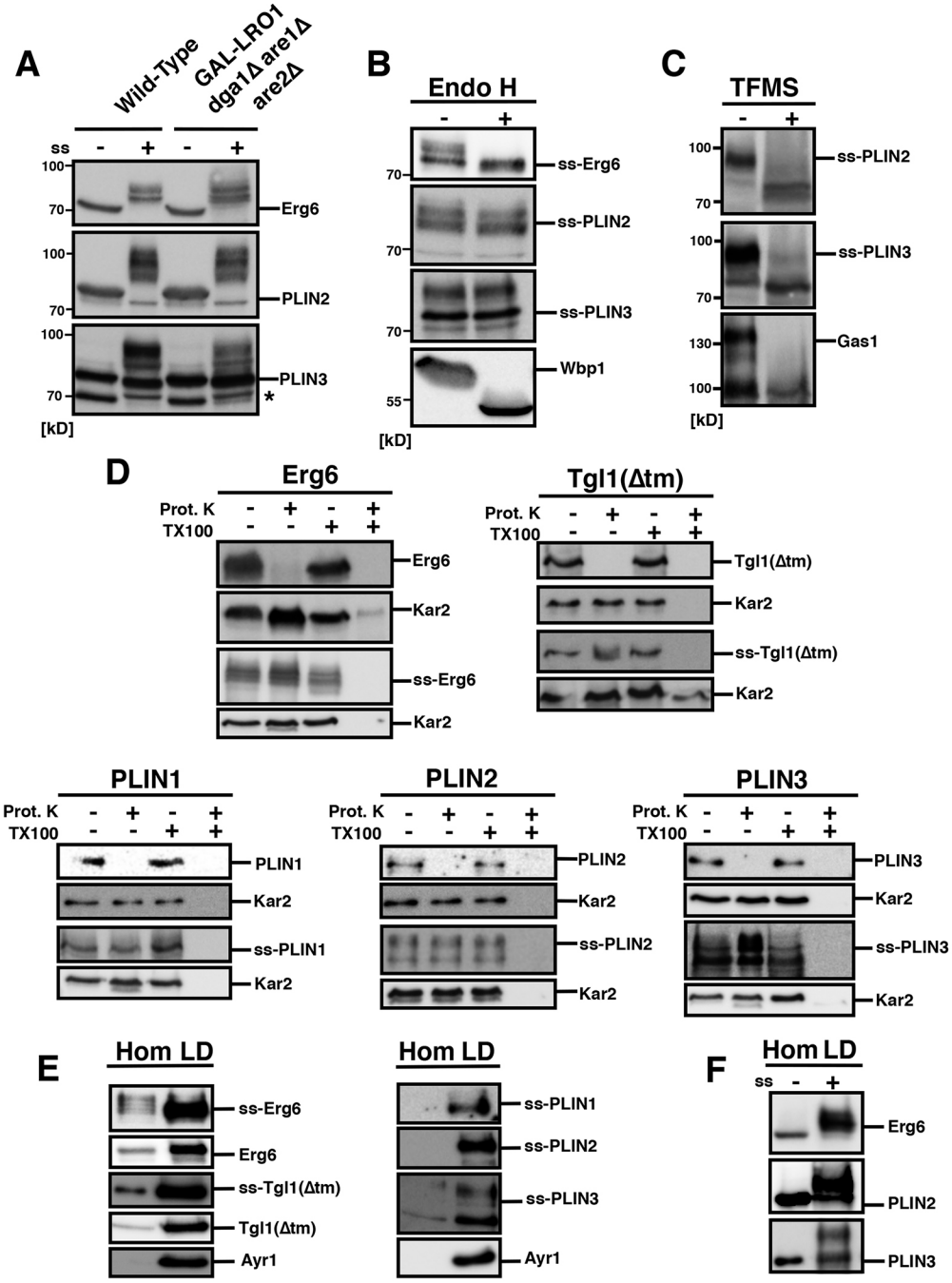

Fig. 3. Signal-sequence-containing lipid droplet marker proteins are glycosylated, protected from digestion by proteinase K and enriched on lipid droplets. (A) Western blot analysis of cytosolic and signal-sequence-containing Erg6, PLIN2 and PLIN3. The band corresponding to the predicted molecular mass of the protein is indicated. The signal-sequence-containing (ss-) proteins run in multiple bands at higher molecular mass. The lower band observed with the cytosolic PLIN3 is likely due to partial degradation of the full-length protein (marked by the star). (B) Endoglycosidase H treatment reduces the apparent molecular mass of ss-Erg6. Protein extracts from cells expressing the indicated proteins were treated with endoglycosidase H (endo H) or left untreated. Proteins were resolved by SDS-PAGE and detected by western blotting. Wbp1, a subunit of the oligosaccharyltransferase complex serves as control for the endo H treatment. (C) Chemical deglycosylation of ss-PLIN2 and ss-PLIN3 reduces their apparent molecular mass. Protein extracts from cells expressing the indicated proteins were treated with trifluoromethanesulphonic acid (TFMS) or left untreated. Gas1, a GPI-anchored surface protein serves as control for the TFMS treatment. (D) Signal-sequence-containing Erg6, Tgl1(Δtm), PLIN1, PLIN2 and PLIN3 are protected from proteinase K (Prot. K) digestion. Microsomes from wild-type cells expressing the indicated proteins were left intact or were treated with Triton X-100 (1%, TX100) and proteinase K for 30 min on ice. Proteins were precipitated with TCA, resolved by SDS-PAGE and detected by western blotting. The ER luminal chaperone Kar2 serves as a control to show that microsomes are intact. (E) Signal-sequence-containing lipid droplet marker proteins are enriched on isolated lipid droplets. Lipid droplets were enriched by subcellular fractionation and equal amounts of proteins (10 µg) of the cell homogenate (Hom) and of the isolated lipid droplet fraction (LD) were separated and analyzed by western blotting. Ayr1 serves as a marker protein for lipid droplets. (F) The glycosylated forms of ss-Erg6, ss-PLIN2 and ss-PLIN3 are enriched on lipid droplets. The migration of tagged proteins from cell-homogenate-containing cytosolic versions of Erg6, PLIN2 and PLIN3 was compared to the migration of the signal-sequence-containing versions of these proteins isolated from lipid droplets by western blotting. Erg6, Tgl1(Δtm) and PLINs were detected using an antibody against GFP; Ayr1, Kar2, Gas1 and Wbp1 were detected using specific antibodies against these proteins.

Journal of Cell Science (2016) 129, 3803-3815 doi:10.1242/jcs.189191

histidinol into histidine and thereby allows *his4* mutant cells to grow on medium containing histidinol. Under standard conditions, this conversion takes place in the cytosol. Therefore, when His4 is targeted to the ER lumen or when it is fused to an ER luminal protein, histidine is not produced. This growth readout thus provides a sensitive assay for the efficiency of translocation and has been used to isolate mutants in the translocon (Deshaies and Schekman, 1987). *his4*Δ cells expressing the dual topology reporter fused C-terminally to the lipid droplet marker proteins containing or lacking the signal sequence were then assayed for growth on histidinol-containing plates. Whereas all the strains expressing the cytosolic versions of the lipid droplet marker proteins were capable of growing on this medium, those expressing the signal-sequence-containing marker proteins and those bearing only an empty plasmid failed to grow even though they all expressed the fusion constructs as monitored by western blotting (Fig. S2A,B).

To further probe the accessibility of the signal-sequence-containing PLINs to cytosolic factors, we introduced a biotinylation site into these reporters. Biotinylation occurs by a cytosolic biotin-CoA ligase and thus inefficient translocation of these reporters into the ER lumen or their retro-translocation into the cytosol, would allow access of the ligase to these reporters resulting in their biotinylation. Detection of biotinylated proteins by western blotting with avidin, revealed that the cytosolic version of PLIN3 is efficiently biotinylated, whereas the signal-sequence-containing PLIN3 was not biotinylated. ss-PLIN3, however, became a substrate for biotinylation when the cell extract was incubated with detergents (1% Triton X-100), an ATP-regenerating system and free biotin for 2 h at 30°C, indicating that the ER luminal version of PLIN3 is a substrate for biotinylation *in vitro* but not *in vivo*, most likely because ss-PLIN3 is shielded from the ligating enzyme by a membrane barrier (Fig. S1B).

To test whether PLINs can penetrate membranes, we targeted PLIN3 to mitochondria by adding the mitochondrial presequence of subunit 9 of the F0 ATPase of *Neurospora crassa* to the N-terminus of GFP–PLIN3. The resulting mito-GFP–PLIN3 fusion colocalized with the mitochondrial marker mito-RFP but not with Nile-Red-stained lipid droplets, indicating that PLIN3 can be targeted and confined to a membrane-enclosed compartment (Fig. S1C).

Signal-sequence-containing PLIN3 localizes to newly formed lipid droplets before these structures are recognized by the cytosolic version of PLIN3

By using an inducible strain in which turning on expression of one of the neutral lipid biosynthetic enzymes, *LRO1*, in a background where the remaining three genes for neutral lipid synthesis are deleted, results in lipid droplet formation, we aimed to assess whether a luminal lipid-droplet-binding protein, such as ss-PLIN3, could be recruited to growing lipid droplets. Therefore, the *GAL-LRO1* strain expressing either cytosolic PLIN3 or ss-PLIN3 was shifted from glucose to galactose medium and the time-dependent formation of lipid droplets was monitored after staining cells with Nile Red. Nile-Red-positive punctate structures were first observed ∼30 min after galactose induction, and the structures then grew in size and number as expression of *LRO1* continued (Fig. 4). Cytosolic PLIN3 was first observed to concentrate over the Nile-Red-positive puncta after 4 h of induction. The ER luminal ss-PLIN3, by contrast, already displayed punctate localization at Nile-Red-positive structures 30 min after induction of *LRO1*, showing that growing lipid droplets are accessible from within the lumen of the ER. In addition, the data also indicate that the ER luminal protein can recognize and concentrate over growing lipid droplets long before these structures become decorated by the corresponding cytosolic lipid-droplet-binding protein, possibly because the concentration of these proteins in the ER lumen is higher than in the cytosol.

Mature lipid droplets are accessible to ER luminal probes

The data so far indicate that ER luminal proteins with a high affinity to lipid droplets can target to lipid droplets but they do not allow to discriminate whether this targeting occurs only at the early stages of lipid droplet biogenesis or whether targeting from within the ER lumen is also possible on lipid droplets that have already been formed. To address this question, we developed a mating-based assay in which one of the mating partners contributes mature lipid droplets that are marked by Erg6–mCherry whereas the other mating partner lacks lipid droplets (*lro1*Δ *dga1*Δ *are1*Δ *are2*Δ) but expresses an ER luminal GFP-tagged ss-PLIN3. At the pre-fusion stage, these two marker proteins do not colocalize, as they are expressed in two separate cells. However, upon cell fusion and subsequent karyogamy, the ER luminal ss-PLIN3 rapidly colocalizes with lipid droplets as evidenced by the line scan at the 15-min time point (Fig. 5A,D). Merging of the ER luminal ss-GFP–PLIN3 onto the pre-existing lipid droplets appeared to occur with a constant rate onto the majority of lipid droplets, indicating that there are no subpopulations of lipid droplets that are shielded from access by the ER luminal probe (Fig. 5B,C). Interestingly, the only outliers shown in the box plot of Fig. 5C are lipid droplets with a high ratio of ss-GFP-PLIN3 to Erg6-mCherry. Visual inspection of these outliers indicate that they are likely due to the formation of new lipid droplets within the part of the ER that originates from the mating partner who originally lacked the respective biosynthetic enzymes, suggesting that these lipid droplets are newly formed during the mating event, probably by movement of the biosynthetic enzymes into the ER of the ss-GFP–PLIN3-expressing mating partner (Fig. S3). Taken together, these data indicate that lipid droplets remain accessible to ER luminal probes even once they have fully matured. The data also excludes the presence of individual cytosolic lipid droplets, as they would be shielded from rapid access by the ER luminal probe.

Expression of ER luminal PLINs does not affect the morphology of lipid droplets or their association with the ER membrane

To examine whether expression of the ER luminal PLINs affects the morphology, membrane structure, or ER association of lipid droplets, we fixed cells expressing either cytosolic or ER luminal versions of PLIN1 or PLIN3 by high-pressure freezing, embedded cells in Spurr's resin, and analyzed their morphology by transmission electron microscopy. Lipid droplets from cells expressing either cytosolic or ER luminal versions of these PLINs appeared as electron translucent structures, characteristic for lipid droplets. Their morphology, however, was indistinguishable from lipid droplets of wild-type cells (Fig. 6; Fig. S4). In all cell types, lipid droplets were frequently observed in close association with the nuclear envelope or with the ER membrane, which appear as electron translucent, ribosome free ribbons, as indicated by the yellow arrows (ER) and arrowheads (nuclear envelope) in Fig. 6 and Fig. S4. On some lipid droplets, ribosome-free zones that appeared to partially or even fully encircle the lipid droplet were observed, indicating that at these places lipid droplets were separated from the bulk of the cytosol (red arrows in Fig. 6, Fig. S4). Whether these ribosome free zones are due to the presence of an additional

Journal of Cell Science (2016) 129, 3803-3815 doi:10.1242/jcs.189191

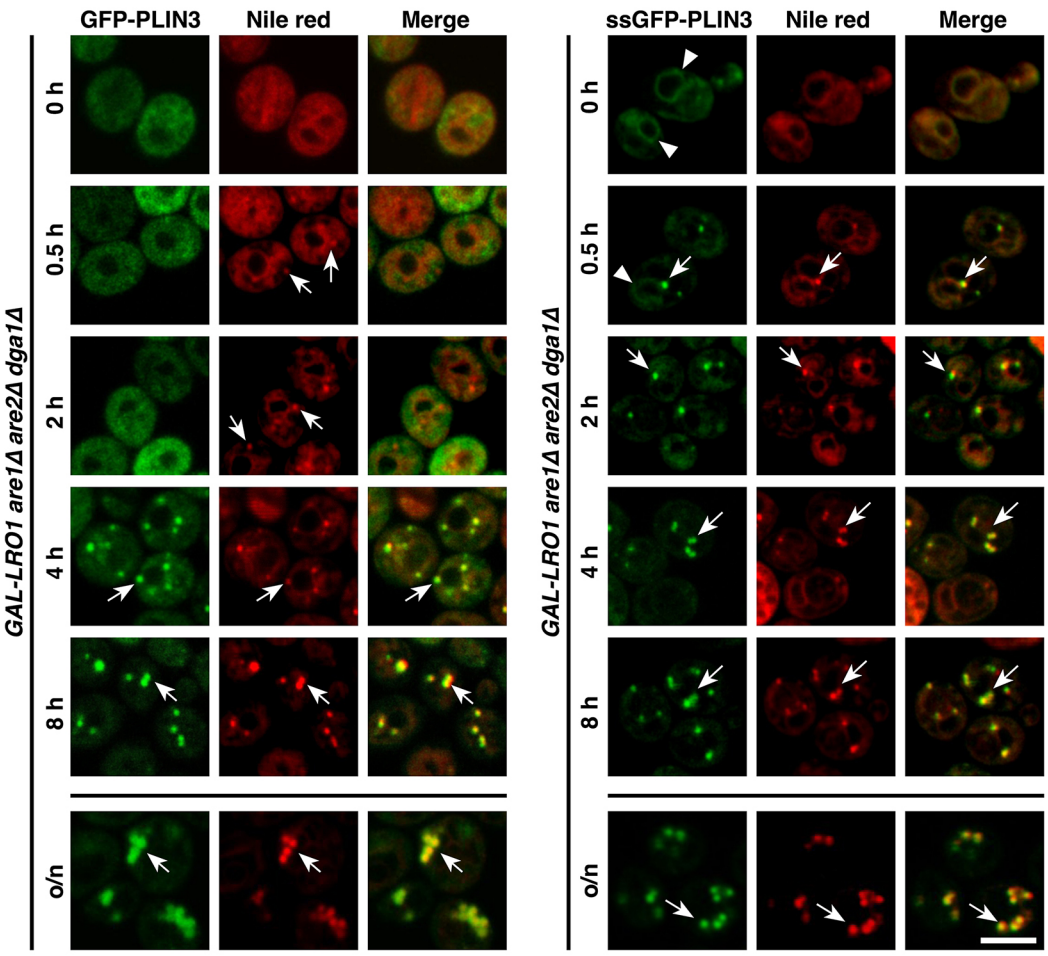

Fig. 4. Both cytosolic and ER luminal versions of PLIN3 localize to newly formed lipid droplets. Cells expressing cytosolic GFP–PLIN3 or the ER luminal ss-GFP–PLIN3 were shifted from glucose- to galactose-containing medium to induce expression of LRO1 and thus to induce lipid droplet formation. Aliquots of cells were removed at the indicated time point or after overnight growth (o/n), stained with Nile Red and analyzed by confocal microscopy. Arrowheads mark the circular ER localization of ss-PLIN3, arrows mark the presence of lipid droplets. Scale bar: 5 µm.

membrane layer, however, cannot unambiguously be resolved from these two-dimensional sections of a possibly complex three-dimension structure. These data thus indicate that the expression of either cytosolic or ER luminal PLINs does not substantially affect the morphology of lipid droplets or their association with the ER membrane, but they cannot conclusively resolve the question as to whether lipid droplets are located inside or only at the ER membrane. The data can also not exclude that expression of ER luminal PLINs could have subtle effects on the topology of lipid droplets that would escape direct visualization by electron microscopy.

Lipid droplets of mammalian cells are accessible to ER luminal proteins

So far we have shown that lipid droplets are accessible to ER luminal lipid-droplet-binding proteins in yeast. To examine whether this is a unique property of yeast lipid droplets, we examined lipid droplet targeting of a signal-sequence-containing PLIN2 protein in mammalian cells. Therefore, we transfected Schwann and HEK293T cells with plasmids expressing cytosolic PLIN2 or with PLIN2 containing an N-terminal signal sequence from BiP (amino acids 1–19; also known as HSPA5), an ER luminal chaperone. GFP–PLIN2 labeled punctate structures and colocalized with mCherry–PLIN2, a construct that has been previously shown to label lipid droplets (Eyre et al., 2014) (Fig. 7A). The signal obtained from the mammalian signal-sequence-containing PLIN2 (mss-GFP–PLIN2) also revealed staining of circular structures; however, the fluorescence signal was weak, suggesting that the protein might be subject to rapid degradation, possibly through ERAD (Xu et al., 2005). Treating cells with the proteasome inhibitor MG132 resulted in improved signal intensity and revealed extensive colocalization of the ER luminal protein with the cytosolic mCherry–PLIN2 over lipid droplets, demonstrating that targeting of ER luminal proteins to lipid droplets is not a unique feature of yeast cells but is also observed in mammalian cells. To confirm that mss-PLIN2 is indeed translocated into the ER lumen we again isolated microsomes and tested accessibility of both cytosolic PLIN2 and mss-PLIN2 to degradation by proteinase K. Whereas the cytosolic version of PLIN2 was readily degraded in the presence of proteinase K, mss-PLIN2 was protected from the protease and degraded only when microsomes were treated with detergents (Fig. 7B). Thus mss-PLIN2 behaved the same as the ER luminal chaperone calreticulin, demonstrating that the protein indeed translocated into the ER lumen. Cytosolic and ER luminal forms of PLIN2 both run as a discrete band with the same electrophoretic mobility, indicating that the ER luminal version of PLIN2 is not subject to glycosylation as is the case in yeast. This difference is likely explained by the fact that O-glycosylation in yeast starts in the ER lumen whereas in higher

Journal of Cell Science (2016) 129, 3803-3815 doi:10.1242/jcs.189191

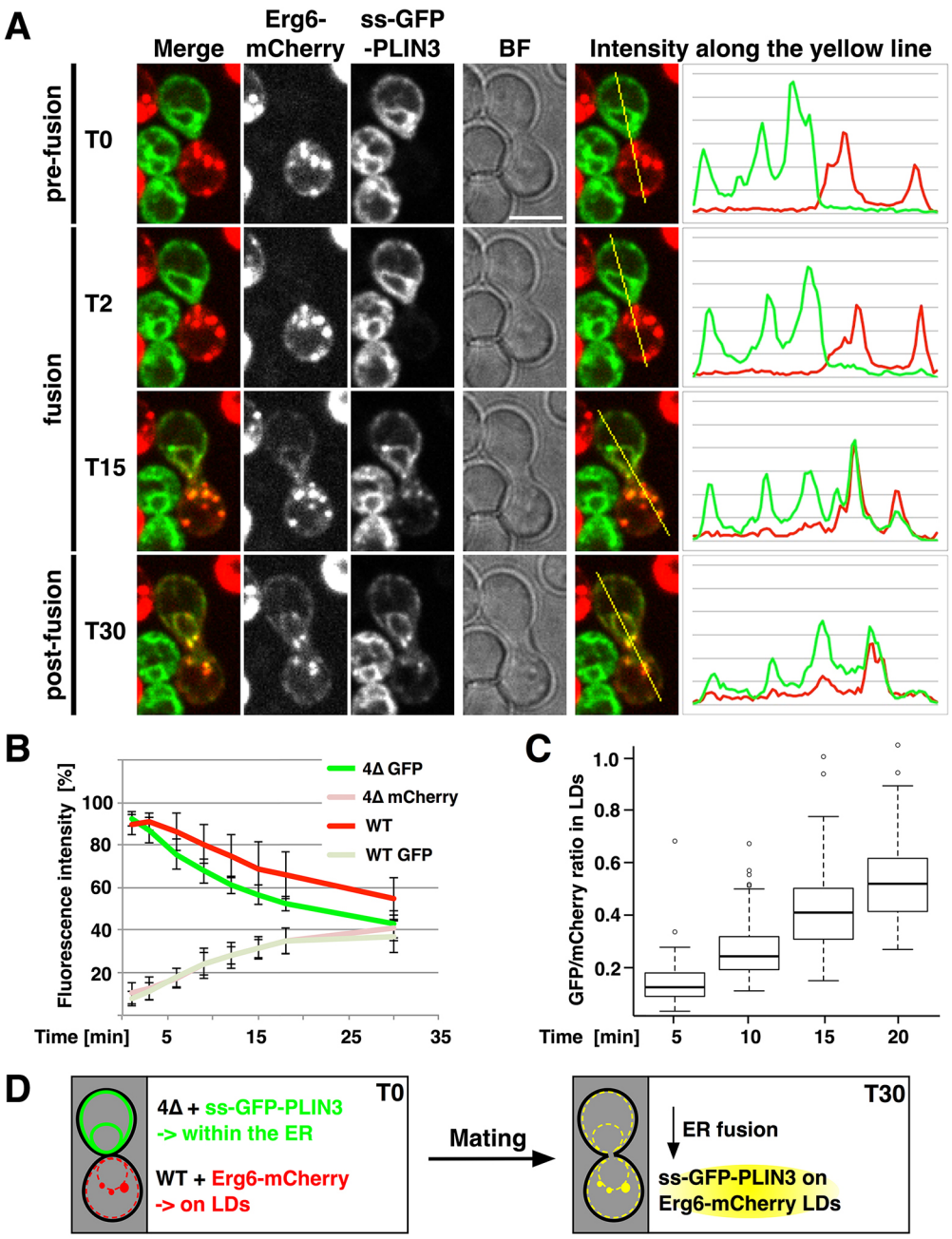

Fig. 5. ER luminal PLIN3 localizes to pre-existing lipid droplets in a yeast mating assay. To test whether the ER luminal PLIN3 can reach mature lipid droplets, exponentially growing MATα 4Δ cells lacking lipid droplets (*lro1Δ dga1Δ are1Δ are2Δ*) and expressing ss-GFP–PLIN3 were mixed 1:1 with wild-type (WT) MATa cells expressing the lipid droplet marker Erg6–mCherry, and incubated for 2 h at 30°C. Cells were then pelleted and mounted on slides with an agar pad for live-cell imaging at 25°C. (A) Mating progression was analyzed by time-lapse spinning disk confocal microscopy with a single confocal section taken every 1 min, and results are displayed over a period of 30 min (T30). Fluorescence intensity profiles along the yellow lines that span the two mating partners are shown in the graphs to the right. BF, bright field image. Scale bar: 5 µm. (B) Fluorescence intensity in both mating partners before fusion is normalized to 100%. The graph displays the time-dependent reduction of the initial fluorescence intensities (red and green lines) and the simultaneous increase of the fluorescence of the newly acquired marker (pale reddish and pale greenish lines) due to movement of the proteins from one cell to the other following mating. Results are mean±s.d. over seven mating events. (C) The rate of transfer of the ER luminal ss-GFP–PLIN3 onto lipid droplets is uniform and constant over time. The ratio between the ER luminal ss-GFP–PLIN3 and Erg6–mCherry at the indicated time points upon cell mating is shown in the box plot. The box represents the 25–75th percentiles, and the median is indicated. The whiskers denote maximum and minimum without outliers (over 1.5-fold from the interquartile range), and the outliers (empty circles) are depicted in the plot. *n*=12 mating events, >105 lipid droplets. (D) Schematic representation of marker protein distribution in yeast cells before and after mating. Merging of the ER luminal marker (ss-GFP–PLIN3) onto lipid droplets marked by Erg6–mCherry upon ER fusion is shown.

eukaryotes this reaction is generally confined to the Golgi (Lommel and Strahl, 2009). These data thus show that lipid droplets of yeast, as well as those of mammalian cells, are accessible from within the lumen of the ER.

DISCUSSION

The results presented here reveal that lipid droplets are accessible from both sides of the ER membrane, that is, from the luminal compartment and from the cytosol. The data thus indicate that lipid

Journal of Cell Science (2016) 129, 3803-3815 doi:10.1242/jcs.189191

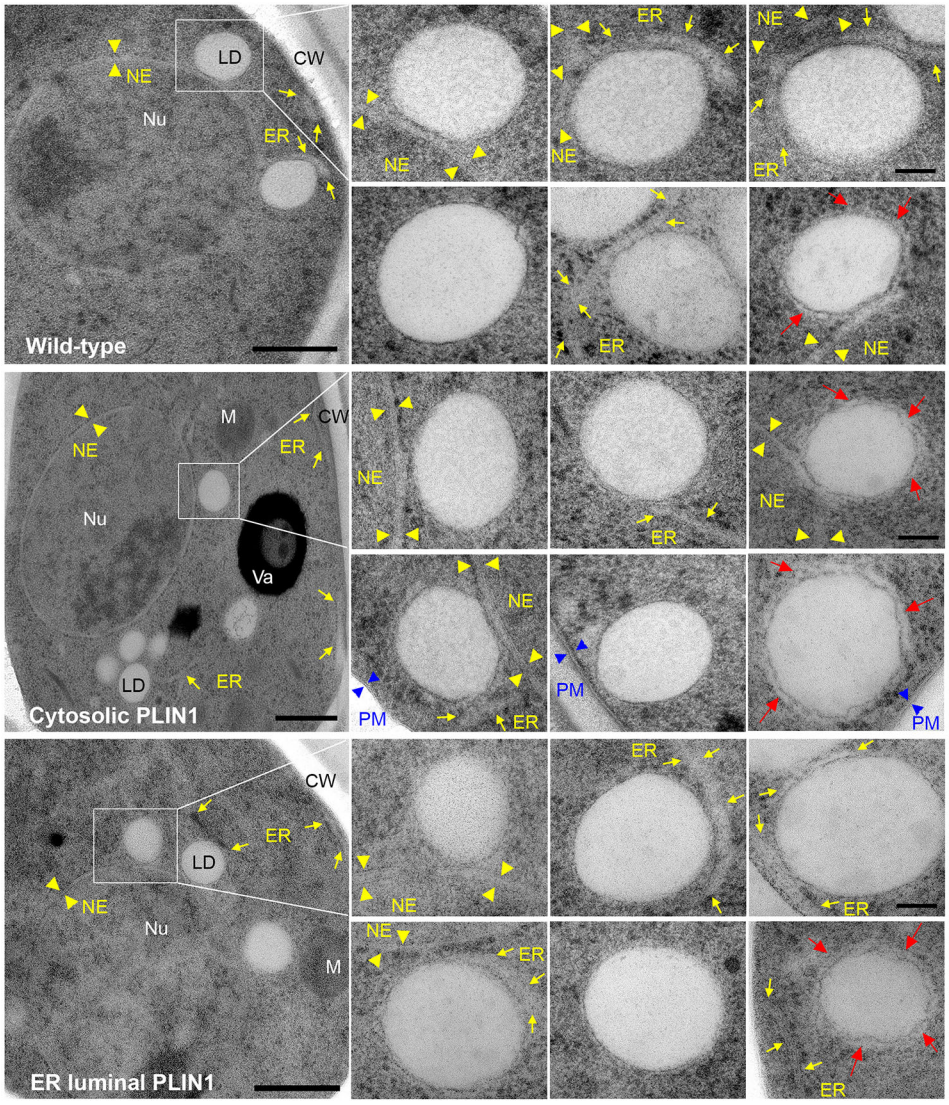

Fig. 6. Expression of ER luminal PLIN1 does not affect the morphology and ER association of lipid droplets. Wild-type cells and cells expressing either cytosolic PLIN1 or ss-PLIN1 were high-pressure cryofixed and processed for electron microscopy. The nuclear envelope (NE) is indicated by yellow arrowheads, the ER is indicated by yellow arrows, the plasma membrane (PM) is indicated by blue arrowheads. Ribosome-free zones covering lipid droplets are indicated by red arrows. LD, lipid droplet; CW, cell wall; M, mitochondria; Nu, nucleus; Va, vacuole. Scale bars: 500 nm (whole cell images on left); 100 nm (magnified views of lipid droplet on the right).

droplets form a domain within the ER that is recognized by proteins that have a high affinity for lipid droplets regardless of whether these proteins are present in the cytosol or within the ER lumen. Although the precise signal that is recognized by lipid-droplet-localized proteins is not yet well defined, it has been speculated that some of these proteins, such as PLIN3, recognize lipid-packaging defects (Bulankina et al., 2009). This is supported by recent results indicating that amphipathic helices present in a number of lipid-droplet-localized proteins, including PLINs, are sufficient for lipid droplet targeting (Grippa et al., 2015; Rowe et al., 2016). Thus, similar to proteins containing lipid-binding amphipathic helices, as present in proteins with an ALPs motif or those of the N-BAR family, which recognize lipid packaging defects induced by membrane curvature, PLIN3 and possibly other lipid-droplet-targeted proteins harboring amphipathic helices, might recognize altered spacing of phospholipid headgroups, possibly induced by the presence of cone-shaped or neutral lipids within a flat bilayer membrane (Bulankina et al., 2009; Drin and Antonny, 2010).

Neutral lipids are soluble to few molar percent within a phospholipid bilayer (Hamilton et al., 1983). They are highly concentrated in the lipid droplet core from where they likely diffuse into the adjacent lipid bilayer and thereby alter the spacing of phospholipid headgroups within the bilayer. The resulting local increase in phospholipid headgroup spacing in turn could be recognized by lipid-droplet-binding proteins containing amphipathic helices. In this scenario, lipid-droplet-binding proteins would thus assemble onto a membrane bilayer enriched in neutral lipids rather than directly onto the monolayer that wraps the hydrophobic core of the lipid droplet.

To account for the observed colocalization of cytosolic and ER luminal lipid droplet proteins, one might postulate that lipid droplets that emanate from the cytosolic leaflet of the ER membrane become encapsulated by an additional layer of ER membrane, resulting in an 'egg cup' arrangement in which the lipid droplets is held in place by the ER membrane similar to a cup holding an egg (Robenek et al., 2006) (Fig. 8A). In this 'egg cup' model, the limiting phospholipid monolayer of the lipid droplet is directly decorated by cytosolic PLINs (red ovals in Fig. 8A), whereas the ER luminal PLINs cover the structure from within the ER extensions that hold the lipid droplet in place (green ovals in Fig. 8A).

Alternatively, if the lens of neutral lipids that is thought to form in the hydrophobic core of the ER bilayer early during lipid droplet biogenesis bends towards the ER lumen rather than towards the cytosol, as is frequently postulated, it could be enwrapped by the ER to yield a structure that would morphologically resemble a lipid droplet in close proximity to the ER, facing the cytosol, as is

Journal of Cell Science (2016) 129, 3803-3815 doi:10.1242/jcs.189191

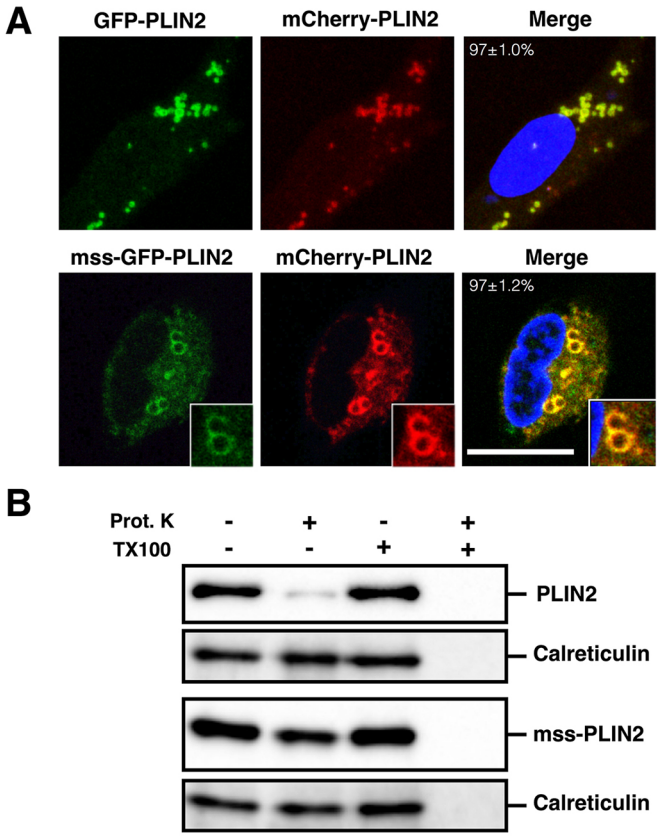

Fig. 7. ER luminal PLIN2 localizes to lipid droplets in mammalian cells. (A) Colocalization of cytosolic PLIN2 and mammalian signal sequence (mss)-PLIN2 in Schwann cells. Cells transfected with plasmids expressing the indicated lipid droplet protein were fixed and analyzed by confocal microscopy. Cells coexpressing mss-GFP–PLIN2 and mCherry–PLIN2 were treated with the proteasome inhibitor MG132 for 6 h prior to fixation. A blow up of a selected region is shown in the inset. DAPI staining is shown in the merge. The degree of colocalization of the two markers is 97±1% (mean±s.e.m., n>400 lipid droplets). Scale bar: 10 µm. (B) mss-PLIN2 is protease protected. Microsomes from HEK293T cells expressing cytosolic or mss-PLIN2 were prepared and incubated with proteinase K for 30 min on ice in the presence or absence of detergent (1% Triton X-100, TX100). The ER luminal chaperone calreticulin serves as a control to show that microsomes are intact.

typically observed by electron microscopy (Fig. 6; Fig. S4; Fig. 8B). Topologically, however, this type of lipid droplet would position its neutral lipid core into the ER lumen, thus allowing direct binding of ER luminal PLINs onto the limiting lipid monolayer (green ovals in Fig. 8B). In this model, cytosolic PLINs could still assemble onto the cytosolic leaflet of the ER membrane, again by recognizing altered lipid spacing induced by the diffusion of triacylglycerol into the confining membrane (red ovals in Fig. 8B). Thus, in this model, lipid droplet biogenesis is topologically identical to the biogenesis of lipoprotein particles, which is initiated by the translocation of a lipoprotein into the ER lumen. This nascent apo-lipoprotein then becomes lipidated by the action of a microsomal triglyceride transfer protein (MTP), an ER luminal protein that forms a complex with protein disulfide isomerase (PDI), and thereby matures into a lipoprotein particle which is secreted into the circulation (Fisher and Ginsberg, 2002; Hussain et al., 2003). In support of such an ER luminal localization of lipid droplets, lipid droplet formation and lipoprotein processing in hepatocytes are two closely linked processes. Apo-lipoprotein B-100 tightly associates with nascent lipid droplets when its degradation is inhibited. This association requires MTP activity and thus occurs between an ER luminal protein and lipid droplets (Ohsaki et al., 2008). Remarkably, immunogold labeling of such arrested apo-lipoproteins reveals that the lipoproteins are separated only by a membrane monolayer from the lipid droplet, the lipid droplet surface is thus directly accessible to an ER luminal protein (Ohsaki et al., 2008).

Both models of lipid droplet biogenesis outlined in Fig. 8 could account for the observed colocalization of cytosolic and ER luminal PLINs. It is interesting to note, however, that lipid droplets have recently been shown to bud into the ER lumen in cells lacking the fat-storage-inducing transmembrane (FIT) proteins (Choudhary et al., 2015). FIT proteins constitute an evolutionary conserved class of ER proteins that bind triacylglycerol *in vitro* and they are important for neutral lipid storage *in vivo* (Gross et al., 2011; Kadereit et al., 2008). Deficiency of FIT2 in the adipose tissue of mice results in progressive lipodystrophy of white adipose depots and metabolic dysfunction (Miranda et al., 2014). In yeast, mouse fibroblasts and *C. elegans*, lack of FIT proteins results in budding of lipid droplets into the ER lumen (Choudhary et al., 2015). This observation has been taken to suggest that FIT proteins are required for budding of lipid droplets from the ER towards the cytosol. An alternative interpretation, however, is that the absence of FIT proteins reveals a process that is morphologically not discernible in their presence. For example, if FIT proteins were important to connect or coordinate the expansion of the lipid droplet monolayer with that of the adjacent ER bilayer, their absence could result in the accumulation of intraluminal lipid droplets, similar to those labeled as ‘nascent stage’ in Fig. 8B.

Both models of lipid droplet biogenesis shown in Fig. 8 postulate stable membrane domains with high curvatures. Stabilizing such highly curved membrane domains is likely to require specialized proteins, such as the hairpin-anchored membrane proteins that are frequently found to localize to lipid droplets and non-bilayer forming lipids. The requirement for such non-bilayer forming lipids might explain why phospholipids from isolated lipid droplets have a distinct fatty acid composition from those of the ER and might also account for the observation that lipid droplet formation in yeast is dependent on the formation of diacylglycerol, a lipid that rapidly flips between membrane leaflets (Adeyo et al., 2011; Schneiter et al., 1999; Tauchi-Sato et al., 2002). The observations reported here that lipid droplets in both yeast and mammalian cells are accessible to ER luminal proteins further support the notion that lipid droplets are closely associated with the ER, and they indicate that this association does not only occur early during lipid droplet biogenesis but that it is likely maintained throughout its lifetime.

MATERIALS AND METHODS

Yeast strains and growth conditions

Yeast strains and their genotypes are listed in Table S1. Double- and triple-mutant strains were generated by crossing of single mutants and by gene disruption, using PCR deletion cassettes and a marker rescue strategy (Gueldener et al., 2002).

GFP tagging and western blot analysis

The signal-sequence-containing reporters were expressed from a pGREG506-based plasmid in which the GAL promoter was replaced by an ADH promoter and the proteins were fused to the *PRY1* ER signal sequence, amino acids 1–19 (Choudhary and Schneiter, 2012). Cloning and expression of PLINs in yeast was performed as previously described (Jacquier et al., 2013). For mammalian expression, we used pLENTI6-mCherry-Plin2 (Eyre et al., 2014) and GFP–PLIN2 and mss-GFP–PLIN2 that were cloned into pSiCoR-GFP-EF1α (Jacob et al., 2014). All constructs were verified by sequencing. Crude lipid droplets were prepared as described previously (Leber et al., 1994).

Journal of Cell Science (2016) 129, 3803-3815 doi:10.1242/jcs.189191

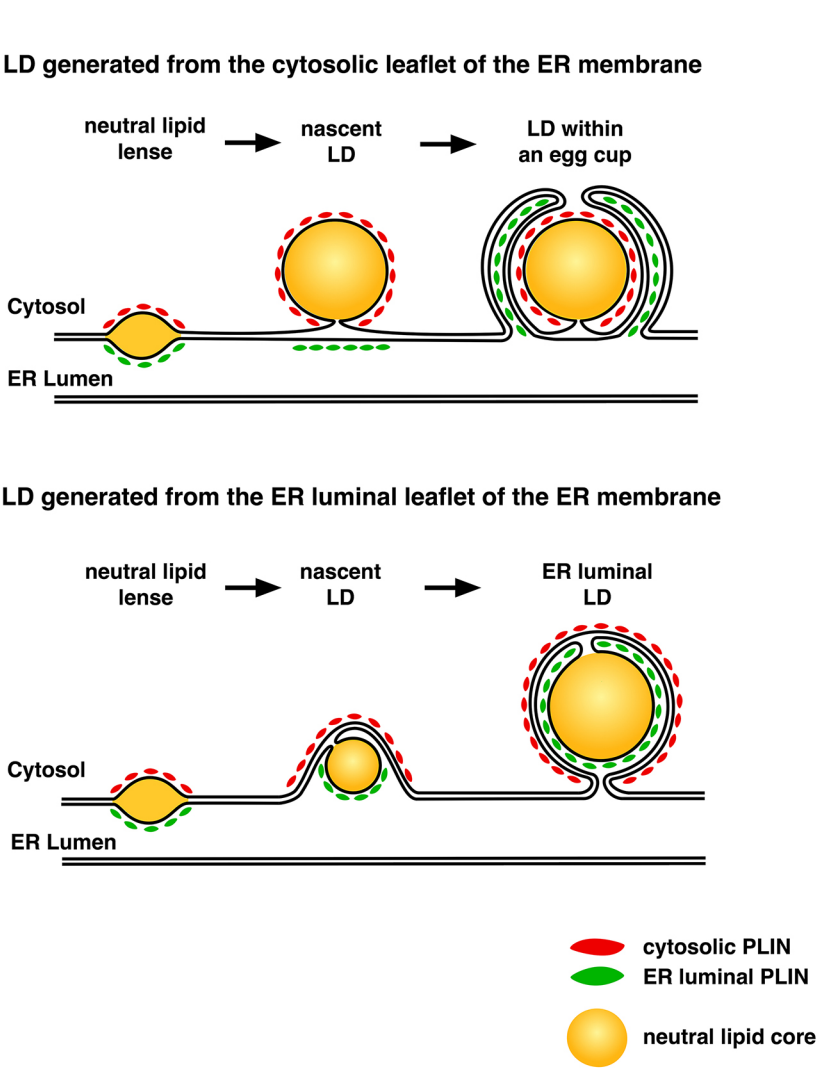

Fig. 8. Models of lipid droplet biogenesis that could account for the colocalization of cytosolic and ER luminal proteins on lipid droplets. (A) Cytosolic lipid droplets (LD) generated by an outward budding of the nascent lipid droplet and held in place by the ER membrane as postulated by the 'egg cup' model. (B) Biogenesis of ER luminal lipid droplets, initiated by budding of a nascent lipid droplet towards the lumen. Cytosolic PLINs are indicated by the red ovals, ER luminal PLINs are indicated by green ovals. The neutral lipid core is indicated in yellow and the ER bilayer is represented by a double line.

Erg6, Tgl1(Δtm) and the PLINs were detected using a monoclonal antibody against GFP (#11814460001, Roche Diagnostics, Rotkreuz, Switzerland, dilution 1:2000). Primary antibodies against Wpb1 (Markus Aebi, ETH Zurich, Switzerland, dilution 1:10,000), Gas1 (Howard Riezman, University of Geneva, Switzerland, dilution 1:2000), Kar2 (Randy Schekman, University of California at Berkeley, CA, dilution 1:5000), Ayr1 (Günther Daum, TU-Graz, Austria, dilution 1:10,000) and calreticulin (Beat Schwaller, University of Fribourg, Switzerland, dilution 1:3000) were detected by using horseradish peroxidase (HRP)-conjugated secondary antibodies (Santa Cruz Biotechnology, Dallas, TX, #sc-2030 and #sc-2302, dilution 1:10,000). Western blots and fractionation experiments were repeated at least two times with essentially similar results.

Proteinase K and endo H treatment were performed as previously described (Tatzer et al., 2002; Choudhary and Schneiter, 2012).

Fluorescence microscopy

Localization of GFP- and mCherry-tagged proteins was performed by fluorescence microscopy of fixed mammalian cells using a Leica TCS SP-II confocal microscope. For living yeast cell imaging, either a Leica TCS SP5 confocal microscope with LAS AF software, a Visitron VisiScope CSU-W1 (Visitron Systems, Puchheim, Germany) or a DeltaVision Elite imaging system (GE Healthcare, Pittsburgh, PA) was used. The Delta Vision Elite imaging system consisted of an Olympus 1X71 inverted microscope equipped with a CCD camera (CoolSNAP HQ^2, Photometrics, Tucson, AZ). Images were acquired with a U PLAN S-APO 100×1.42 NA oil immersion objective (Olympus) and a GFP or mCherry filter set. Six to eight 0.2 µm optical sections were deconvolved using the iterative constrained deconvolution program in softWoRx (Applied Precision). Single sections are displayed. Confocal images produced with the Leica TCS SP5 microscope were recorded with an APO 40×1.3 NA or an APO 63×1.3 NA oil immersion objectives (Leica) with a zoom of 6 or 3, respectively. The Visitron spinning disk CSU-W1 consisted of a Nikon Ti-E inverted microscope, equipped with a CSU-W1 spinning disk head with a 50-µm pinhole disk (Yokogawa, Tokyo, Japan), an Evolve 512 (Photometrics) EM-CCD camera, and a PLAN APO 100× NA 1.3 oil objective (Nikon). Live cells were stained with Nile Red (10 mg/ml, Sigma-Aldrich, St Louis, MO) for 1 min at room temperature and washed twice with PBS. Quantification of the GFP and mCherry signals was performed using Fiji software (Schindelin et al., 2012). Colocalization was assessed manually by counting the number of lipid droplets per cells that were stained by the GFP- and mCherry-tagged marker proteins. The rate of fluorescent protein transfer onto lipid droplets upon mating was calculated from maximal intensity projections of seven confocal sections spaced by 0.6 µm. Data were analyzed using R (version 3.2.5). All microscopic experiments were performed at least two times with essentially similar results.

Expression and localization of PLINs in mammalian cells

HEK293T cells (ATCC) were grown in DMEM (Gibco) containing 10% fetal bovine serum (Biochrom) and 0.2% penicillin-streptomycin (Gibco). Purified primary rat Schwann cell cultures were obtained and grown as described previously (Jacob et al., 2008). For immunofluorescence, Schwann cells were treated 48 h after transfection with 10 µM MG132 for 6 h, washed with PBS, fixed with 4% paraformaldehyde for 15 min at room temperature,

washed again in PBS, incubated for 30 min in 0.3% Triton X-100 in PBS and 5 min in DAPI in PBS, and mounted in Citifluor (Agar Scientific). Microsomes were prepared from HEK293T cells and protease protection assays were performed as described previously (Kaznacheyeva et al., 1998).

Dual topology reporter and mitochondrial targeting

The respective genes were amplified either with or without the signal sequence from Pry1 (amino acids 1–19) and cloned into pJK90 by homologous recombination in strain STY50. Plasmid pJK90 contains the *OST4* gene, three HA tags, part of the *SUC2* gene and *HIS4C* (Kim et al., 2003a). Growth assays and western blots of dual topology reporters were repeated two times with similar results.

To target GFP–PLIN3 into mitochondria, PLIN3 was cloned into pVT100U, which contains the first 69 amino acids of subunit 9 of the F0 ATPase of *Neurospora crassa* as a mitochondrial presequence (Westermann and Neupert, 2000).

Biotinylation assays

The biotinylatable versions of cytosolic PLIN3 were generated by amplifying the biotin acceptor peptide from YEpURA-CUP1-HBTubiquitin (Tagwerker et al., 2006) and cloning into SpeI-linearized pGREG576ADH-GFP-PLIN3 (Jacquier et al., 2013). The biotinylatable version of the ER luminal ss-GFP–PLIN3 was generated by PCR ligation of the biotin acceptor site from YEpURA-CUP1-HBTubiquitin and GFP–PLIN3 from pGREG576-ADH-GFP-PLIN3. All plasmids were verified by sequencing.

For *in vitro* biotinylation, cells were disrupted with glass beads in lysis buffer (100 mM $NaPO_4$, pH 7.5, 0.2 M sorbitol, 5 mM $MgCl_2$, 2 mM PMSF and 1% Triton X-100). 50 µg of cell extracts was incubated for 2 h at 30°C in the presence of biotin (100 µM), CoA (500 µM) and an ATP-regenerating system (75 mM phosphocreatine, 5 mM ADP, 10 mM ATP, 10 mM $MgCl_2$ and 25 units creatine phosphokinase). The biotinylation assay was repeated two times with similar results.

Electron microscopy

For cryofixation, mid-log phase cells were transferred into lecithin-treated 0.1 mm deep Leica membrane carriers and frozen by high-pressure freezing (Studer et al., 2001). The frozen specimens were freeze-substituted in acetone containing 2% osmium tetroxide (EMS, Hatfield, PA), 0.1% uranyl acetate (EMS), 1% methanol and 3% water (AFS, Leica-Microsystems) (Walther and Ziegler, 2002). The substitution protocol was as follows: −90°C for 27 h, −60°C for 8 h and −30°C for another 8 h. The samples were then washed four times for 30 min in 100% acetone, warmed up to room temperature and embedded in Spurr's resin (through a series of 30%, 50%, 70% and 2×100%). Blocks were polymerized at 60°C for 5 days. Ultrathin sections (75 nm) were collected on formvar-coated grids, post stained with uranyl acetate and lead citrate, visualized with a FEI Tecnai Spirit TEM (Hillsboro, OR), and images were recorded on a FEI Eagle CCD camera and processed with Photoshop.

Acknowledgements

We thank members of the laboratory for their support, suggestions and comments on the manuscript, A. Conzelmann for discussions and comments on the manuscript, A. Puoti for localizing ss-PLINs in nematodes, O. Duman for help with the mammalian cell culture, and M. Beard, A. Conzelmann, J. Nunnari, M. Rose and B. Schwaller, for reagents. Electron microscopy sample preparation and imaging were performed with devices supported by the Microscopy Imaging Center (MIC) of the University of Bern.

Competing interests

The authors declare no competing or financial interests.

Author contributions

Conceptualization, S.M., R.K., S.C., V.S., C.J. and R.S.; Formal Analysis, R.K., S.C. and C.J.; Investigation, S.M., R.K., S.C., V.S. and C.J.; Writing, C.J. and R.S., Visualization, S.M., R.K., S.C., V.S. and C.J.; Supervision, C.J. and R.S.; Funding acquisition, C.J. and R.S.

Funding

This work was supported by the Canton of Fribourg; and by the Schweizerischer Nationalfonds zur Förderung der Wissenschaftlichen Forschung (Swiss National Science Foundation).

Supplementary information

Supplementary information available online at
http://jcs.biologists.org/lookup/doi/10.1242/jcs.189191.supplemental

References

Adeyo, O., Horn, P. J., Lee, S., Binns, D. D., Chandrahas, A., Chapman, K. D. and Goodman, J. M. (2011). The yeast lipin orthologue Pah1p is important for biogenesis of lipid droplets. *J. Cell Biol.* **192**, 1043-1055.

Athenstaedt, K. and Daum, G. (2000). 1-Acyldihydroxyacetone-phosphate reductase (Ayr1p) of the yeast Saccharomyces cerevisiae encoded by the open reading frame YIL124w is a major component of lipid particles. *J. Biol. Chem.* **275**, 235-240.

Barbosa, A. D., Savage, D. B. and Siniossoglou, S. (2015). Lipid droplet-organelle interactions: emerging roles in lipid metabolism. *Curr. Opin. Cell Biol.* **35**, 91-97.

Bickel, P. E., Tansey, J. T. and Welte, M. A. (2009). PAT proteins, an ancient family of lipid droplet proteins that regulate cellular lipid stores. *Biochim. Biophys. Acta Mil. Cell Biol. Lipids* **1791**, 419-440.

Blanchette-Mackie, E. J., Dwyer, N. K., Barber, T., Coxey, R. A., Takeda, T., Rondinone, C. M., Theodorakis, J. L., Greenberg, A. S. and Londos, C. (1995). Perilipin is located on the surface layer of intracellular lipid droplets in adipocytes. *J. Lipid Res.* **36**, 1211-1226.

Bulankina, A. V., Deggerich, A., Wenzel, D., Mutenda, K., Wittmann, J. G., Rudolph, M. G., Burger, K. N. J. and Honing, S. (2009). TIP47 functions in the biogenesis of lipid droplets. *J. Cell Biol.* **185**, 641-655.

Carvalho, P., Goder, V. and Rapoport, T. A. (2006). Distinct ubiquitin-ligase complexes define convergent pathways for the degradation of ER proteins. *Cell* **126**, 361-373.

Choudhary, V. and Schneiter, R. (2012). Pathogen-Related Yeast (PRY) proteins and members of the CAP superfamily are secreted sterol-binding proteins. *Proc. Natl. Acad. Sci. USA* **109**, 16882-16887.

Choudhary, V., Jacquier, N. and Schneiter, R. (2011). The topology of the triacylglycerol synthesizing enzyme Lro1 indicates that neutral lipids can be produced within the luminal compartment of the endoplasmatic reticulum: implications for the biogenesis of lipid droplets. *Commun. Integr. Biol.* **4**, 781-784.

Choudhary, V., Ojha, N., Golden, A. and Prinz, W. A. (2015). A conserved family of proteins facilitates nascent lipid droplet budding from the ER. *J. Cell Biol.* **211**, 261-271.

Czabany, T., Athenstaedt, K. and Daum, G. (2007). Synthesis, storage and degradation of neutral lipids in yeast. *Biochim. Biophys. Acta Mol. Cell Biol. Lipids* **1771**, 299-309.

Deshaies, R. J. and Schekman, R. (1987). A yeast mutant defective at an early stage in import of secretory protein precursors into the endoplasmic reticulum. *J. Cell Biol.* **105**, 633-645.

Drin, G. and Antonny, B. (2010). Amphipathic helices and membrane curvature. *FEBS Lett.* **584**, 1840-1847.

Eyre, N. S., Fiches, G. N., Aloia, A. L., Helbig, K. J., McCartney, E. M., McErlean, C. S. P., Li, K., Aggarwal, A., Turville, S. G. and Beard, M. R. (2014). Dynamic imaging of the hepatitis C virus NS5A protein during a productive infection. *J. Virol.* **88**, 3636-3652.

Fisher, E. A. and Ginsberg, H. N. (2002). Complexity in the secretory pathway: the assembly and secretion of apolipoprotein B-containing lipoproteins. *J. Biol. Chem.* **277**, 17377-17380.

Grippa, A., Buxó, L., Mora, G., Funaya, C., Idrissi, F.-Z., Mancuso, F., Gomez, R., Muntanyà, J., Sabidó, E. and Carvalho, P. (2015). The seipin complex Fld1/Ldb16 stabilizes ER-lipid droplet contact sites. *J. Cell Biol.* **211**, 829-844.

Gross, D. A., Zhan, C. and Silver, D. L. (2011). Direct binding of triglyceride to fat storage-inducing transmembrane proteins 1 and 2 is important for lipid droplet formation. *Proc. Natl. Acad. Sci. USA* **108**, 19581-19586.

Gueldener, U., Heinisch, J., Koehler, G. J., Voss, D. and Hegemann, J. H. (2002). A second set of loxP marker cassettes for Cre-mediated multiple gene knockouts in budding yeast. *Nucleic Acids Res.* **30**, e23.

Hamilton, J. A., Miller, K. W. and Small, D. M. (1983). Solubilization of triolein and cholesteryl oleate in egg phosphatidylcholine vesicles. *J. Biol. Chem.* **258**, 12821-12826.

Hussain, M. M., Shi, J. and Dreizen, P. (2003). Microsomal triglyceride transfer protein and its role in apoB-lipoprotein assembly. *J. Lipid Res.* **44**, 22-32.

Jacob, C., Grabner, H., Atanasoski, S. and Suter, U. (2008). Expression and localization of Ski determine cell type-specific TGFbeta signaling effects on the cell cycle. *J. Cell Biol.* **182**, 519-530.

Jacob, C., Lötscher, P., Engler, S., Baggiolini, A., Varum Tavares, S., Brügger, V., John, N., Büchmann-Møller, S., Snider, P. L., Conway, S. J. et al. (2014). HDAC1 and HDAC2 control the specification of neural crest cells into peripheral glia. *J. Neurosci.* **34**, 6112-6122.

Jacquier, N., Choudhary, V., Mari, M., Toulmay, A., Reggiori, F. and Schneiter, R. (2011). Lipid droplets are functionally connected to the endoplasmic reticulum in Saccharomyces cerevisiae. *J. Cell Sci.* **124**, 2424-2437.

Jacquier, N., Mishra, S., Choudhary, V. and Schneiter, R. (2013). Expression of oleosin and perilipins in yeast promotes formation of lipid droplets from the endoplasmic reticulum. *J. Cell Sci.* **126**, 5198-5209.
Kadereit, B., Kumar, P., Wang, W.-J., Miranda, D., Snapp, E. L., Severina, N., Torregroza, I., Evans, T. and Silver, D. L. (2008). Evolutionarily conserved gene family important for fat storage. *Proc. Natl. Acad. Sci. USA* **105**, 94-99.
Kassan, A., Herms, A., Fernandez-Vidal, A., Bosch, M., Schieber, N. L., Reddy, B. J. N., Fajardo, A., Gelabert-Baldrich, M., Tebar, F., Enrich, C. et al. (2013). Acyl-CoA synthetase 3 promotes lipid droplet biogenesis in ER microdomains. *J. Cell Biol.* **203**, 985-1001.
Kaznacheyeva, E., Lupu, V. D. and Bezprozvanny, I. (1998). Single-channel properties of inositol (1,4,5)-trisphosphate receptor heterologously expressed in HEK-293 cells. *J. Gen. Physiol.* **111**, 847-856.
Kim, H., Melen, K. and von Heijne, G. (2003a). Topology models for 37 Saccharomyces cerevisiae membrane proteins based on C-terminal reporter fusions and predictions. *J. Biol. Chem.* **278**, 10208-10213.
Kim, H., Yan, Q., Von Heijne, G., Caputo, G. A. and Lennarz, W. J. (2003b). Determination of the membrane topology of Ost4p and its subunit interactions in the oligosaccharyltransferase complex in Saccharomyces cerevisiae. *Proc. Natl. Acad. Sci. USA* **100**, 7460-7464.
Koffel, R., Tiwari, R., Falquet, L. and Schneiter, R. (2005). The Saccharomyces cerevisiae YLL012/YEH1, YLR020/YEH2, and TGL1 genes encode a novel family of membrane-anchored lipases that are required for steryl ester hydrolysis. *Mol. Cell. Biol.* **25**, 1655-1668.
Leber, R., Zinser, E., Paltauf, F., Daum, G. and Zellnig, G. (1994). Characterization of lipid particles of the yeast, Saccharomyces cerevisiae. *Yeast* **10**, 1421-1428.
Lommel, M. and Strahl, S. (2009). Protein O-mannosylation: conserved from bacteria to humans. *Glycobiology* **19**, 816-828.
Markgraf, D. F., Klemm, R. W., Junker, M., Hannibal-Bach, H. K., Ejsing, C. S. and Rapoport, T. A. (2014). An ER protein functionally couples neutral lipid metabolism on lipid droplets to membrane lipid synthesis in the ER. *Cell Rep.* **6**, 44-55.
Miranda, D. A., Kim, J.-H., Nguyen, L. N., Cheng, W., Tan, B. C., Goh, V. J., Tan, J. S. Y., Yaligar, J., Kn, B. P., Velan, S. S. et al. (2014). Fat storage-inducing transmembrane protein 2 is required for normal fat storage in adipose tissue. *J. Biol. Chem.* **289**, 9560-9572.
Miura, S., Gan, J.-W., Brzostowski, J., Parisi, M. J., Schultz, C. J., Londos, C., Oliver, B. and Kimmel, A. R. (2002). Functional conservation for lipid storage droplet association among Perilipin, ADRP, and TIP47 (PAT)-related proteins in mammals, Drosophila, and Dictyostelium. *J. Biol. Chem.* **277**, 32253-32257.
Murphy, S., Martin, S. and Parton, R. G. (2009). Lipid droplet-organelle interactions; sharing the fats. *Biochim Biophys Acta Mol. Cell Biol. Lipids* **1791**, 441-447.
Ohsaki, Y., Cheng, J., Suzuki, M., Fujita, A. and Fujimoto, T. (2008). Lipid droplets are arrested in the ER membrane by tight binding of lipidated apolipoprotein B-100. *J. Cell Sci.* **121**, 2415-2422.
Ohsaki, Y., Suzuki, M. and Fujimoto, T. (2014). Open questions in lipid droplet biology. *Chem. Biol.* **21**, 86-96.
Pol, A., Gross, S. P. and Parton, R. G. (2014).Biogenesis of the multifunctional lipid droplet: lipids, proteins, and sites. *J. Cell Biol.* **204**, 635-646.
Robenek, H., Hofnagel, O., Buers, I., Robenek, M. J., Troyer, D. and Severs, N. J. (2006). Adipophilin-enriched domains in the ER membrane are sites of lipid droplet biogenesis. *J. Cell Sci.* **119**, 4215-4224.
Rogers, J. V., McMahon, C., Baryshnikova, A., Hughson, F. M. and Rose, M. D. (2014). ER-associated retrograde SNAREs and the Dsl1 complex mediate an alternative, Sey1p-independent homotypic ER fusion pathway. *Mol. Biol. Cell* **25**, 3401-3412.
Rowe, E. R., Mimmack, M. L., Barbosa, A. D., Haider, A., Isaac, I., Ouberai, M. M., Thiam, A. R., Patel, S., Saudek, V., Siniossoglou, S. et al. (2016). Conserved amphipathic helices mediate lipid droplet targeting of perilipins 1-3. *J. Biol. Chem.* **291**, 6664-6678.
Sandager, L., Gustavsson, M. H., Stahl, U., Dahlqvist, A., Wiberg, E., Banas, A., Lenman, M., Ronne, H. and Stymne, S. (2002). Storage lipid synthesis is non-essential in yeast. *J. Biol. Chem.* **277**, 6478-6482.
Schindelin, J., Arganda-Carreras, I., Frise, E., Kaynig, V., Longair, M., Pietzsch, T., Preibisch, S., Rueden, C., Saalfeld, S., Schmid, B. et al. (2012). Fiji: an open-source platform for biological-image analysis. *Nat. Methods* **9**, 676-682.
Schneiter, R., Brugger, B., Sandhoff, R., Zellnig, G., Leber, A., Lampl, M., Athenstaedt, K., Hrastnik, C., Eder, S., Daum, G. et al. (1999). Electrospray ionization tandem mass spectrometry (ESI-MS/MS) analysis of the lipid molecular species composition of yeast subcellular membranes reveals acyl chain-based sorting/remodeling of distinct molecular species en route to the plasma membrane. *J. Cell Biol.* **146**, 741-754.
Sorger, D., Athenstaedt, K., Hrastnik, C. and Daum, G. (2004). A yeast strain lacking lipid particles bears a defect in ergosterol formation. *J. Biol. Chem.* **279**, 31190-31196.
Studer, D., Graber, W., Al-Amoudi, A. and Eggli, P. (2001). A new approach for cryofixation by high-pressure freezing. *J. Microsc.* **203**, 285-294.
Szymanski, K. M., Binns, D., Bartz, R., Grishin, N. V., Li, W.-P., Agarwal, A. K., Garg, A., Anderson, R. G. W. and Goodman, J. M. (2007). The lipodystrophy protein seipin is found at endoplasmic reticulum lipid droplet junctions and is important for droplet morphology. *Proc. Natl. Acad. Sci. USA* **104**, 20890-20895.
Tagwerker, C., Flick, K., Cui, M., Guerrero, C., Dou, Y., Auer, B., Baldi, P., Huang, L. and Kaiser, P. (2006). A tandem affinity tag for two-step purification under fully denaturing conditions: application in ubiquitin profiling and protein complex identification combined with in vivocross-linking. *Mol. Cell. Proteomics.* **5**, 737-748.
Targett-Adams, P., Chambers, D., Gledhill, S., Hope, R. G., Coy, J. F., Girod, A. and McLauchlan, J. (2003). Live cell analysis and targeting of the lipid droplet-binding adipocyte differentiation-related protein. *J. Biol. Chem.* **278**, 15998-16007.
Tatzer, V., Zellnig, G., Kohlwein, S. D. and Schneiter, R. (2002). Lipid-dependent subcellular relocalization of the acyl chain desaturase in yeast. *Mol. Biol. Cell* **13**, 4429-4442.
Tauchi-Sato, K., Ozeki, S., Houjou, T., Taguchi, R. and Fujimoto, T. (2002). The surface of lipid droplets is a phospholipid monolayer with a unique Fatty Acid composition. *J. Biol. Chem.* **277**, 44507-44512.
Thiam, A. R., Farese, R. V., Jr and Walther, T. C. (2013). The biophysics and cell biology of lipid droplets. *Nat. Rev. Mol. Cell Biol.* **14**, 775-786.
Walther, P. and Ziegler, A. (2002). Freeze substitution of high-pressure frozen samples: the visibility of biological membranes is improved when the substitution medium contains water. *J. Microsc.* **208**, 3-10.
Westermann, B. and Neupert, W. (2000). Mitochondria-targeted green fluorescent proteins: convenient tools for the study of organelle biogenesis in Saccharomyces cerevisiae. *Yeast* **16**, 1421-1427.
Wilfling, F., Wang, H., Haas, J. T., Krahmer, N., Gould, T. J., Uchida, A., Cheng, J.-X., Graham, M., Christiano, R., Frohlich, F. et al. (2013). Triacylglycerol synthesis enzymes mediate lipid droplet growth by relocalizing from the ER to lipid droplets. *Dev. Cell* **24**, 384-399.
Xu, G., Sztalryd, C., Lu, X., Tansey, J. T., Gan, J., Dorward, H., Kimmel, A. R. and Londos, C. (2005). Post-translational regulation of adipose differentiation-related protein by the ubiquitin/proteasome pathway. *J. Biol. Chem.* **280**, 42841-42847.
Xu, L., Zhou, L. and Li, P. (2012a). CIDE proteins and lipid metabolism. *Arterioscler. Thromb. Vasc. Biol.* **32**, 1094-1098.
Xu, N., Zhang, S. O., Cole, R. A., McKinney, S. A., Guo, F., Haas, J. T., Bobba, S., Farese, R. V., Jr and Mak, H. Y. (2012b). The FATP1-DGAT2 complex facilitates lipid droplet expansion at the ER-lipid droplet interface. *J. Cell Biol.* **198**, 895-911.
Zehmer, J. K., Bartz, R., Bisel, B., Liu, P., Seemann, J. and Anderson, R. G. W. (2009). Targeting sequences of UBXD8 and AAM-B reveal that the ER has a direct role in the emergence and regression of lipid droplets. *J. Cell Sci.* **122**, 3694-3702.

Supplementary Material

Supplementary Figures

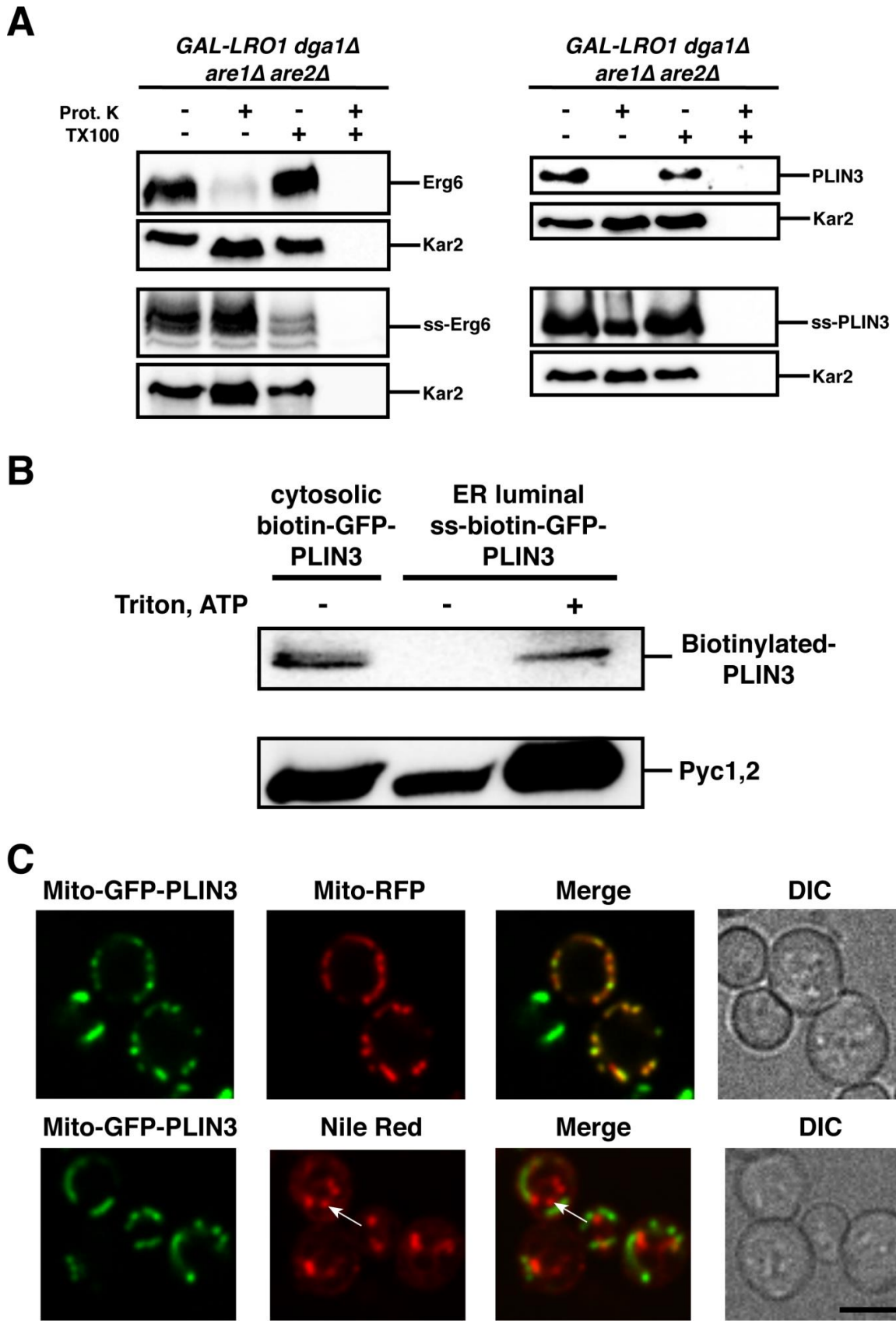

Figure S1. ss-containing marker proteins are protease protected in cells lacking LDs, protected from biotinylation, and PLIN3 can efficiently be targeted to mitochondria.

A) ss-Erg6 and ss-PLIN3 are protease protected when expressed in cells lacking LDs. Cells of the indicated genotype were cultivated in glucose containing medium, microsomes were isolated and subjected to digestion by proteinase K (Prot. K) in the presence and absence of Triton X-100 (TX100). Proteins were separated by SDS-PAGE and Western blots were probed with antibodies against GFP and Kar2. B) A signal sequence containing biotinylatable PLIN3 is protected from biotinylation by the cytosolic biotin-CoA ligase *in vivo*. Cell extracts were prepared from cells expressing a cytosolic or signal sequence containing biotinylatable version of PLIN3. Where indicated, the extract was incubated for 2 h at 30°C with 1% Triton X-100, with free biotin, CoA, and an ATP regenerating system. Proteins were then separated by SDS-PAGE and biotinylated proteins were detected with avidin conjugated to horseradish peroxidase. The native, biotinylated protein pyruvate carboxylase Pyc1,2 (130 kD) serves as a loading control. C) PLIN3 containing a mitochondrial targeting signal colocalizes with the mitochondrial marker mito-RFP but not with LDs. Cells expressing GFP-PLIN3, containing an N-terminal mitochondrial targeting signal, were analyzed by confocal microscopy. Colocalization was observed between the fusion protein and the mitochondria marker mito-RFP, but not between mito-GFP-PLIN3 and Nile red-stained LDs. Bar, 5 µm.

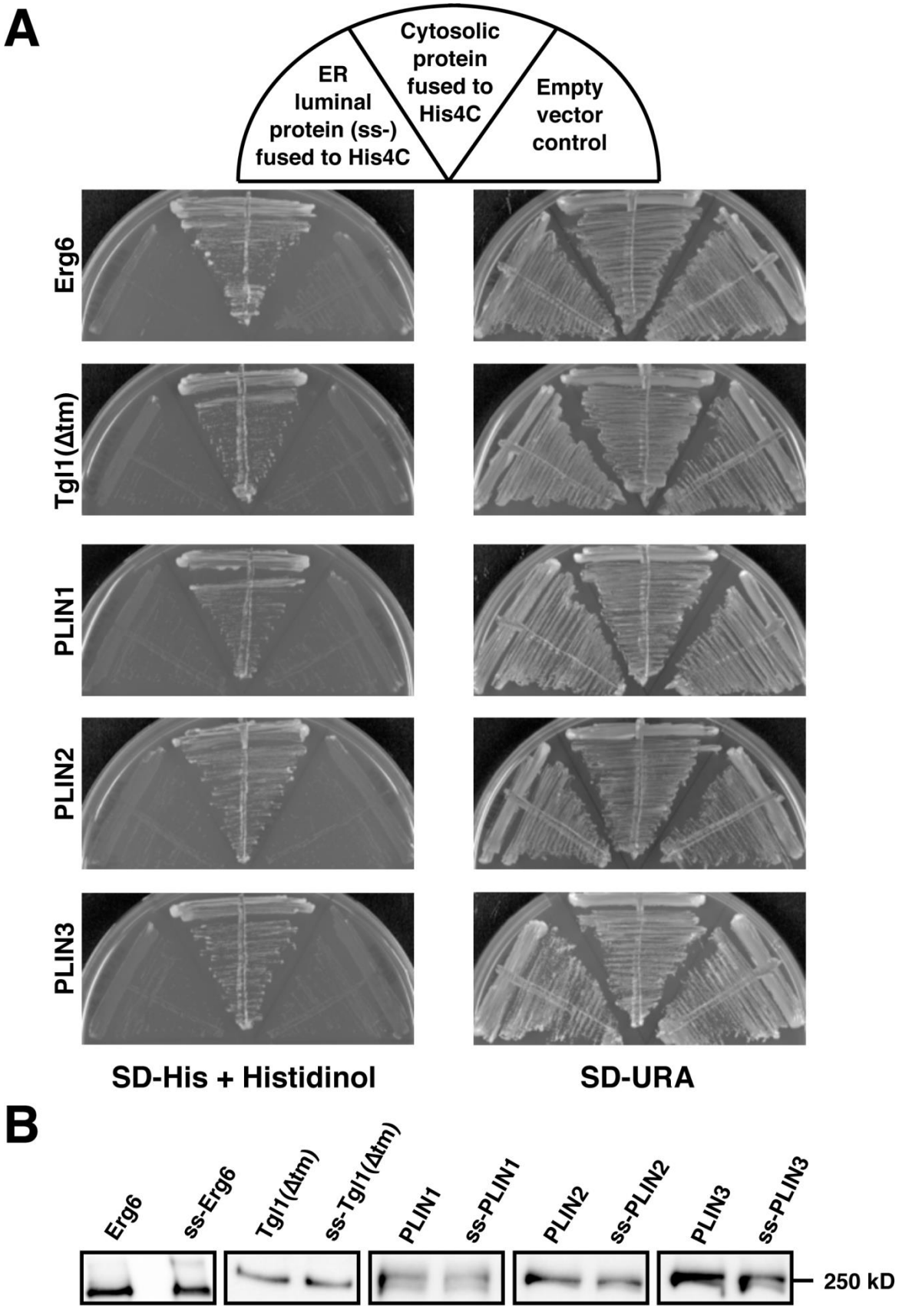

Figure S2. Signal sequence containing LD marker proteins are stringently translocated.

A) Histidine auxotrophic cells expressing the indicated LD marker proteins fused to the invertase-His4C dual topology reporter were streaked on plates lacking histidine but containing histidinol and on plates lacking uracil to control for the presence of the plasmid. Absence of growth is consistent with an ER luminal localization of the respective fusion protein. B) The dual topology reporters are expressed. Western blot using an antibody against GFP showing expression of the cytosolic and ss-containing variants of the indicated LD marker proteins.

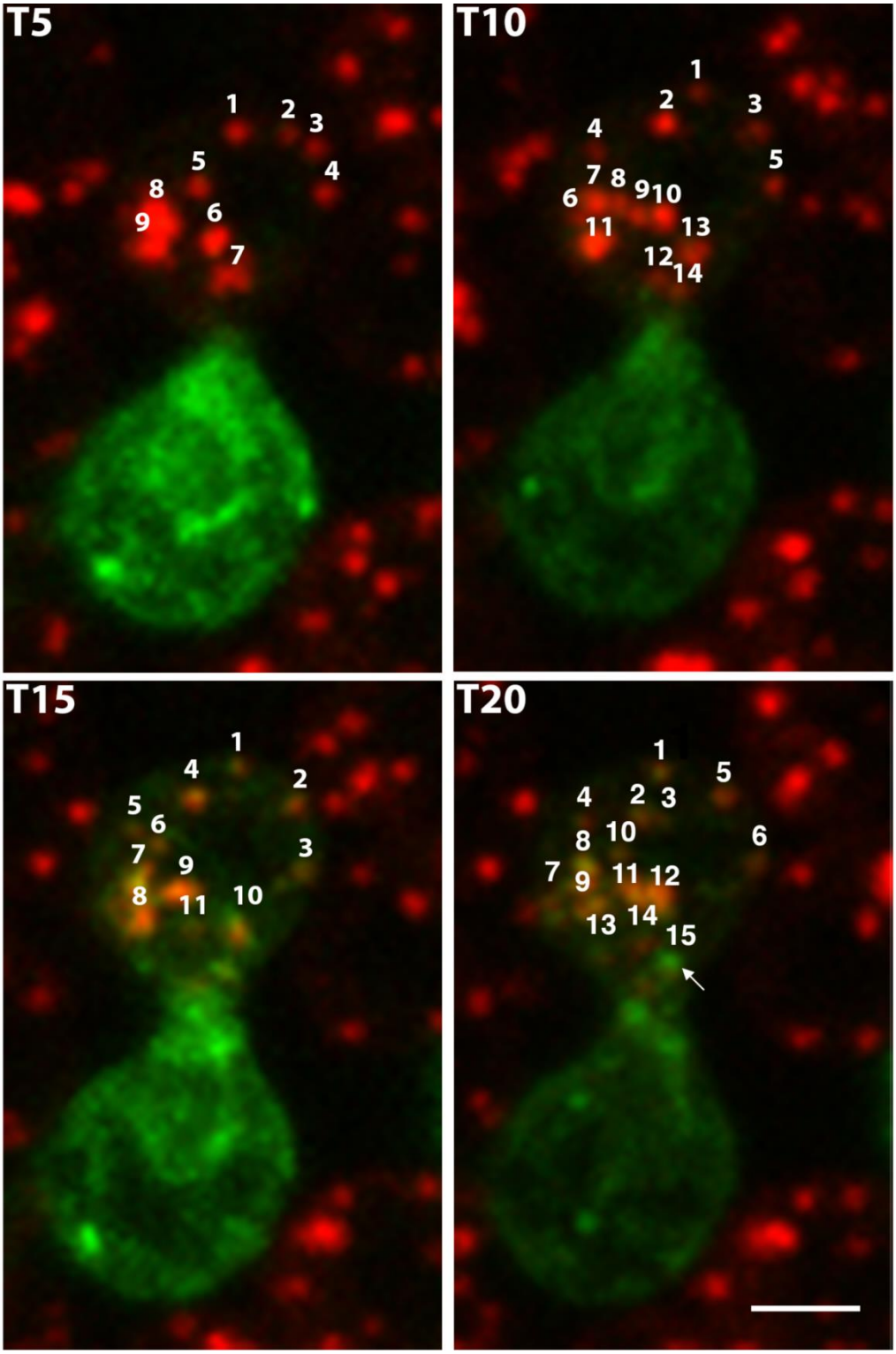

Figure S3. Quantification of the rate of ss-GFP-PLIN3 onto LDs marked by Erg6-mCherry upon cell fusion.

MATα 4Δ cells lacking LDs (*lro1*Δ *dga1*Δ *are1*Δ *are2*Δ) expressing ss-GFP-PLIN3 were mated with wild-type MATa cells expressing the LD marker Erg6-mCherry, and mating progression was analyzed by time-lapse spinning disk confocal microscopy with 7 confocal sections, separated by 0.6 µm, taken every 1 min. Maximal intensity projections from the 5, 10, 15, and 20 min time points are displayed. GFP and mCherry intensities of every LD were normalized to the total GFP and mCherry intensities present in the respective mating partner. Individual LDs are numbered to measure the ratio of GFP/mCherry fluorescence. An outliner with a high GFP/mCherry ratio at the T20 time point is indicated by the arrow. Bar, 2 µm.

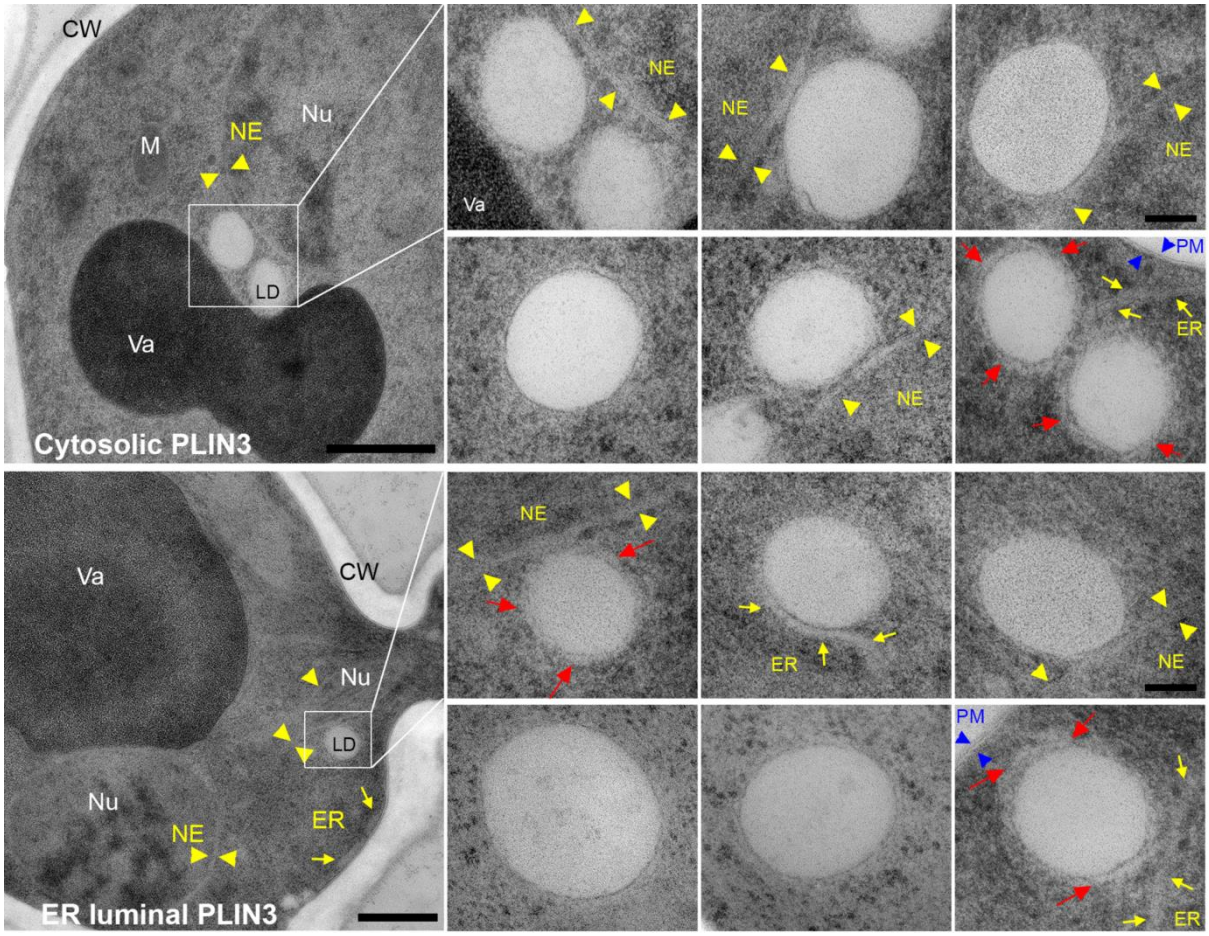

Figure S4. Expression of ER luminal PLIN3 does not affect the morphology and ER association of LDs.

Cells expressing either cytosolic PLIN3 or ss-PLIN3 were cryofixed and processed for EM. The nuclear envelope (NE) is indicated by yellow arrowheads, the ER is indicated by yellow arrows, the plasma membrane (PM) is indicated by blue arrowheads. Ribosome free zones covering LDs are indicated by red arrows. CW, cell wall; M, mitochondria; Nu, nucleus; Va, vacuole. Bar in whole cell images, 500 nm; in LD blow ups, 100 nm.

Table S1: Yeast strains used in this study

Name	Relevant Genotype	Source
RSY1533	*MATα his3Δ1 leu2Δ0 lys2Δ0 ura3Δ0*	Euroscarf
RSY5226	*MATα his3Δ1 leu2Δ0 lys2Δ0 ura3Δ0 pGREG506-ADH1-ERG6-GFP-URA3*	This study
RSY5361	*MATα his3Δ1 leu2Δ0 lys2Δ0 ura3Δ0 pRS416-ADH1-TGL1$^{30-548}$-GFP-URA3*	This study
RSY5305	*MATα his3Δ1 leu2Δ0 lys2Δ0 ura3Δ0 pGREG506-ADH1-SS^{PRY1}-ERG6-GFP-URA3*	This study
RSY5360	*MATα his3Δ1 leu2Δ0 lys2Δ0 ura3Δ0 pRS416-ADH1-SS^{PRY1}-TGL1$^{30-548}$-GFP-URA3*	This study
RSY4640	*MATα his3Δ1 leu2Δ0 lys2Δ0 ura3Δ0 pGREG576-ADH1-GFP-PLIN1-URA3*	Jacquier *et al.*, 2013
RSY4639	*MATα his3Δ1 leu2Δ0 lys2Δ0 ura3Δ0 pGREG576-ADH1-GFP-PLIN2-URA3*	Jacquier *et al.*, 2013
RSY4647	*MATα his3Δ1 leu2Δ0 lys2Δ0 ura3Δ0 pGREG576-ADH1-GFP-PLIN3-URA3*	Jacquier *et al.*, 2013
RSY5470	*MATα his3Δ1 leu2Δ0 lys2Δ0 ura3Δ0 pGREG506-ADH1-SS^{PRY1}-GFP-PLIN1-URA3*	This study
RSY5525	*MATα his3Δ1 leu2Δ0 lys2Δ0 ura3Δ0 pRS416-ADH1-SS^{PRY1}-GFP-PLIN2-URA3*	This study
RSY5472	*MATα his3Δ1 leu2Δ0 lys2Δ0 ura3Δ0 pGREG506-ADH1-SS^{PRY1}-GFP-PLIN3-URA3*	This study
RSY3021	*MATα his3Δ1 leu2Δ0 lys2Δ0 ura3Δ0 trp1Δ0 GAL-LRO1::TRP1 dga1::loxP are1::KanMX are2::KanMX*	Lab collection
RSY4645	*MATα his3Δ1 leu2Δ0 lys2Δ0 ura3Δ0 trp1Δ0 GAL-LRO1::TRP1 dga1::loxP are1::KanMX are2::KanMX pGREG576-ADH1-GFP-PLIN2-URA3*	Jacquier *et al.*, 2013
RSY5729	*MATα his3Δ1 leu2Δ0 lys2Δ0 ura3Δ0 trp1Δ0 GAL-LRO1::TRP1 dga1::loxP are1::KanMX are2::KanMX pRS416-ADH1-SS^{PRY1}-GFP-*	This study

	PLIN2-URA3	
RSY4641	*MATα his3Δ1 leu2Δ0 lys2Δ0 ura3Δ0 trp1Δ0 GAL-LRO1::TRP1 dga1::loxP are1::KanMX are2::KanMX pGREG576-ADH1-GFP-PLIN3-URA3*	Jacquier *et al.*, 2013
RSY5306	*MATα his3Δ1 leu2Δ0 lys2Δ0 ura3Δ0 trp1Δ0 GAL-LRO1::TRP1 dga1::loxP are1::KanMX are2::KanMX pGREG506-ADH1-SS^{PRY1}-ERG6-GFP-URA3*	This study
RSY5308	*MATα his3Δ1 leu2Δ0 lys2Δ0 ura3Δ0 trp1Δ0 GAL-LRO1::TRP1 dga1::loxP are1::KanMX are2::KanMX pGREG506-ADH1-SS^{PRY1}-GFP-PLIN3-URA3*	This study
RSY5718	*MATα his3Δ1 leu2Δ0 lys2Δ0 ura3Δ0 trp1Δ0 GAL-LRO1::TRP1 dga1::loxP are1::KanMX are2::KanMX pGREG506-ADH1-ERG6-GFP-URA3*	This study
RSY5715	*MATα his3Δ1 leu2Δ0 lys2Δ0 ura3Δ0 trp1Δ0 GAL-LRO1::TRP1 dga1::loxP are1::KanMX are2::KanMX HRD1::HIS3*	This study
RSY5717	*MATα his3Δ1 leu2Δ0 lys2Δ0 ura3Δ0 pGREG506-ADH1-SS^{PRY1}-ERG6-GFP-URA3 pGREG503-ADH1-ERG6-mCherry-HIS3*	This study
RSY5719	*MATα his3Δ1 leu2Δ0 lys2Δ0 ura3Δ0 trp1Δ0 GAL-LRO1::TRP1 dga1::loxP are1::KanMX are2::KanMX pGREG506-ADH1-ERG6-GFP-URA3 pADH-mCherryHDEL-LEU2::CEN*	This study
RSY5720	*MATα his3Δ1 leu2Δ0 lys2Δ0 ura3Δ0 trp1Δ0 GAL-LRO1::TRP1 dga1::loxP are1::KanMX are2::KanMX pGREG506-ADH1-SS^{PRY1}-ERG6-GFP-URA3 pADH-mCherryHDEL-LEU2::CEN*	This study
RSY5721	*MATα his3Δ1 leu2Δ0 lys2Δ0 ura3Δ0 trp1Δ0 GAL-LRO1::TRP1 dga1::loxP are1::KanMX are2::KanMX pRS416-ADH1-TGL1$^{30-548}$-GFP-URA3 pADH-mCherryHDEL-LEU2::CEN*	This study

RSY5722	*MATα his3Δ1 leu2Δ0 lys2Δ0 ura3Δ0 trp1Δ0 GAL-LRO1::TRP1 dga1::loxP are1::KanMX are2::KanMX pRS416-ADH1- SS^{PRY1}-TGL1$^{30-548}$-GFP-URA3 pADH-mCherryHDEL-LEU2::CEN*	This study
RSY5723	*MATα his3Δ1 leu2Δ0 lys2Δ0 ura3Δ0 trp1Δ0 GAL-LRO1::TRP1 dga1::loxP are1::KanMX are2::KanMX pGREG576-ADH1-GFP-PLIN1-URA3 pADH-mCherryHDEL-LEU2::CEN*	This study
RSY5724	*MATα his3Δ1 leu2Δ0 lys2Δ0 ura3Δ0 trp1Δ0 GAL-LRO1::TRP1 dga1::loxP are1::KanMX are2::KanMX pGREG576-ADH1- SS^{PRY1}-GFP-PLIN1-URA3 pADH-mCherryHDEL-LEU2::CEN*	This study
RSY5725	*MATα his3Δ1 leu2Δ0 lys2Δ0 ura3Δ0 trp1Δ0 GAL-LRO1::TRP1 dga1::loxP are1::KanMX are2::KanMX pGREG576-ADH1-GFP-PLIN3-URA3 pADH-mCherryHDEL-LEU2::CEN*	This study
RSY5726	*MATα his3Δ1 leu2Δ0 lys2Δ0 ura3Δ0 trp1Δ0 GAL-LRO1::TRP1 dga1::loxP are1::KanMX are2::KanMX pGREG576-ADH1- SS^{PRY1}-GFP-PLIN3-URA3 pADH-mCherryHDEL-LEU2::CEN*	This study
RSY5727	*MATα his3Δ1 leu2Δ0 lys2Δ0 ura3Δ0 trp1Δ0 GAL-LRO1::TRP1 dga1::loxP are1::KanMX are2::KanMX hrd1::HIS3 pRS416-ADH1-GFP-PLIN2-URA3 pADH-mCherryHDEL-LEU2::CEN*	This study
RSY5728	*MATα his3Δ1 leu2Δ0 lys2Δ0 ura3Δ0 trp1Δ0 GAL-LRO1::TRP1 dga1::loxP are1::KanMX are2::KanMX hrd1::HIS3 pRS416-ADH1-SS^{PRY1}-GFP-PLIN2-URA3 pADH-mCherryHDEL-LEU2::CEN*	This study
RSY5531	*MATα his4-401 leu2-3 trp1-1 ura3-52 HOL1-1 SUC2::LEU2*	A. Conzelmann
RSY5521	*MATα his4-401 leu2-3 trp1-1 ura3-52 HOL1-1 SUC2::LEU2 pJK90-TPI-ERG6-3(HA)-SUC2-HIS4C-URA3*	This study
RSY5522	*MATα his4-401 leu2-3 trp1-1 ura3-52 HOL1-1 SUC2::LEU2 pJK90-TPI-TGL1(30-548)-3(HA)-SUC2-HIS4C-URA3*	This study
RSY5520	*MATα his4-401 leu2-3 trp1-1 ura3-52 HOL1-1 SUC2::LEU2 pJK90-TPI-GFP-PLIN1-3(HA)-*	This study

	SUC2-HIS4C-URA3	
RSY5518	*MATα his4-401 leu2-3 trp1-1 ura3-52 HOL1-1 SUC2::LEU2 pJK90-TPI-GFP-PLIN2-3(HA)-SUC2-HIS4C-URA3*	This study
RSY5519	*MATα his4-401 leu2-3 trp1-1 ura3-52 HOL1-1 SUC2::LEU2 pJK90-TPI-GFP-PLIN3-3(HA)-SUC2-HIS4C-URA3*	This study
RSY5597	*MATα his4-401 leu2-3 trp1-1 ura3-52 HOL1-1 SUC2::LEU2 pJK90-TPI-SS^{PRY1}-GFP-PLIN1-3(HA)-SUC2-HIS4C-URA3*	This study
RSY5598	*MATα his4-401 leu2-3 trp1-1 ura3-52 HOL1-1 SUC2::LEU2 pJK90-TPI-SS^{PRY1}-GFP-PLIN2-3(HA)-SUC2-HIS4C-URA3*	This study
RSY5599	*MATα his4-401 leu2-3 trp1-1 ura3-52 HOL1-1 SUC2::LEU2 pJK90-TPI-SS^{PRY1}-GFP-PLIN3-3(HA)-SUC2-HIS4C-URA3*	This study
RSY5464	*MATα his4-401 leu2-3 trp1-1 ura3-52 HOL1-1 SUC2::LEU2 pJK90-TPI-SS^{PRY1}-ERG6-3(HA)-SUC2-HIS4C-URA3*	This study
RSY5736	*MATα his4-401 leu2-3 trp1-1 ura3-52 HOL1-1 SUC2::LEU2 pJK90-TPI-SS^{PRY1}-TGL1(30-548)-3(HA)-SUC2-HIS4C-URA3*	This study
RSY5809	*MATα his3Δ1 leu2Δ0 lys2Δ0 ura3Δ0 pGREG576-ADH1-Biotin-GFP-PLIN3-URA3*	This study
RSY5810	*MATα his3Δ1 leu2Δ0 lys2Δ0 ura3Δ0 pRS416-ADH1-SS^{PRY1}-Biotin-GFP-PLIN3-URA3*	This study
RSY5741	*MATα his3Δ1 leu2Δ0 lys2Δ0 ura3Δ0 pVT100U-mito-GFP-PLIN3-URA3*	This study
RSY5807	*MATα his3Δ1 leu2Δ0 lys2Δ0 ura3Δ0 pVT100U-mito-GFP-PLIN3-URA3 pMito-RFP-LEU*	This study
RSY5811	*MATa his3Δ1 leu2Δ0 met15Δ0 ura3Δ p503-ADH1-Erg6-mCherry-HIS3*	This study
RSY5812	*MATα his3Δ1 leu2Δ0 lys2Δ0 ura3Δ are1::KanMX are2::KanMX dga1::KanMX lro1::KanMX pGREG506-ADH1-SS^{PRY1}-PLIN3-URA3*	This study